The University of
Nottingham

UNITED KINGDOM · CHINA · MALAYSIA

Tuttle, William D. and Gardner, Adrian M. and O'Regan, Kieran B. and Malewicz, William and Wright, Timothy G. (2017) Vibrational and vibrational-torsional interactions in the 0–600 cm-1 region of the S1 □ S0 spectrum of p-xylene investigated with resonance-enhanced multiphoton ionization (REMPI) and zero-kinetic-energy (ZEKE) spectroscopy. Journal of Chemical Physics . ISSN 1089-7690 (In Press)

Access from the University of Nottingham repository:

http://eprints.nottingham.ac.uk/40677/3/pXyl_Low_E_vibs-SUBMIT%20%28Tuttle%29.pdf

Vibrational and vibrational-torsional interactions in the 0–600 cm^{-1} region of the S$_1$ ← S$_0$ spectrum of *p*-xylene investigated with resonance-enhanced multiphoton ionization (REMPI) and zero-kinetic-energy (ZEKE) spectroscopy

William D. Tuttle, Adrian M Gardner, Kieran B. O'Regan, William Malewicz, and Timothy G. Wright[a]

Email: Tim.Wright@nottingham.ac.uk

School of Chemistry, University of Nottingham, University Park, Nottingham NG7 2RD UK

Abstract

We assign the 0–600 cm^{-1} region of the S$_1$ ← S$_0$ transition in *p*-xylene using resonance-enhanced multiphoton ionization (REMPI) and zero-kinetic-energy (ZEKE) spectroscopy. In the 0–300 cm^{-1} range, as well as the intense origin band there are a number of torsional and vibration-torsion (vibtor) features. The latter are discussed in more detail in an accompanying paper [Gardner et al. J. Chem. Phys. XXX, xxxxxx (2016)]. Here we focus on the origin and the 300–650 cm^{-1} region, where vibrational bands and some vibtor activity is observed. From the origin ZEKE spectrum we derive the ionization energy of *p*-xylene as 68200 ± 5 cm^{-1}. The assignment of the REMPI spectrum is based on the activity observed in the ZEKE spectra coupled with knowledge of the vibrational wavenumbers obtained from quantum chemical calculations. We assign several isolated vibrations, and a complex Fermi resonance that is found to comprise contributions from both vibrations and vibtor levels, and we examine this via a two-dimensional ZEKE (2D-ZEKE) spectrum. A number of the vibrational features in the REMPI and ZEKE spectra of *p*-xylene that have been reported previously are reassigned and now largely consist of totally-symmetric contributions. We briefly discuss the appearance of non-Franck-Condon allowed transitions. Finally, we find remarkably similar spectral activity to that in the related disubstituted benzenes, *para*-difluorobenzene and *para*-fluorotoluene.

I. INTRODUCTION

Molecules that contain methyl groups are, of course, prevalent in nature. As such, the recognition that methyl groups are key to understanding various photophysical phenomena in such molecules makes fundamental studies on simple molecules that contain this group particularly pertinent. This has been highlighted by Parmenter and coworkers for *p*-fluorotoluene (see reference 1 and subsequent work by the same group).

In previous work, our group, also in collaboration with that of K. L. Reid, has studied the toluene molecule;[2,3] in addition, the importance of doorway states and their identification has been emphasised,[4] building on work on *p*-fluorotoluene (*p*FT) by Davies and Reid.[5] The studies involved complementary information obtained from resonance-enhanced multiphoton ionization (REMPI) spectroscopy, zero-kinetic-energy (ZEKE) spectroscopy and time-resolved photoelectron spectroscopy (tr-PES) experiments. We note particularly that a complex Fermi resonance (one involving more than two vibrational zero order states, ZOSs) was observed at ~460 cm^{-1} and was concluded to involve three ZOSs, M_{11}, M_{14}^2 and $M_{19}M_{20}$ (the vibrational nomenclature is that of ref. 6); to slightly higher energy was a band assigned to a combination of the M_{18} vibration with a torsional level (we term such vibration-torsional states "vibtor" states hereafter). This complex Fermi resonance (FR) feature has been investigated by REMPI and ZEKE spectroscopy,[2] by two-dimensional laser-induced fluorescence (2D-LIF)[7] and tr-PES.[8] Each of these has provided complementary information concerning the contributing ZOSs of the Fermi resonance.

Recent work by Lawrance and coworkers on toluene[9,10] has re-emphasised earlier conclusions on the role of methyl groups in the acceleration of intramolecular energy redistribution, a more-general form of intermolecular vibrational redistribution (IVR) via vibration-torsional coupling. IVR is important since the rapid dispersal of energy within a molecule is an important way by which dissociation can be avoided – particularly pertinent to biomolecules in relation to photostability – see, for example, refs 11 and 12. Clearly a detailed understanding of IVR requires a detailed knowledge of the energy level structure in different molecules; in particular, knowledge of the atomic motion will underpin models of how interaction of vibrations with torsional motion occurs.

In the present work, consisting of the present paper and ref. 13, we present analysis of the 0–600 cm^{-1} region of the REMPI spectrum of the symmetrically disubstituted molecule, *p*-xylene (*p*Xyl), which has two methyl groups located on opposite sides of the phenyl ring. The presence of a second substituent modifies the vibrations significantly, in the same way that the vibrations of monosubstituted benzenes are significantly different to those of benzene;[6] this affects both the form of the vibrations as well as their wavenumbers. We have recently examined the vibrations of *para*-disubstituted benzenes[14] and put forward D_i labels for these, which we shall employ in the present work. This will be seen to be particularly useful in the present work, owing to: errors and inconsistencies in, and inappropriateness of the use of Wilson[15] or Varsányi[16] labels; the fact that we wish to compare activity across the *p*FT, *p*DFB and *p*Xyl molecules, which have different symmetries, and so different Mulliken[17] (Herzberg[18]) numberings; and the confusion arising from the previous (inappropriate) inclusion of methyl-localized vibrations in the C_{2v} Mulliken labels associated with *p*FT in a number of publications.

Herein, we examine the $S_1 \leftarrow S_0$ electronic transition in *p*Xyl using REMPI and ZEKE spectroscopy. Except for the origin, we have discussed the 0–300 cm^{-1} region in a separate publication,[13] just noting here that this region consists of torsion and vibtor transitions. We shall initially discuss the ZEKE spectrum recorded via the $S_1 \leftarrow S_0$ origin, and then move onto the 300–600 cm^{-1} section of the spectrum, which contains a number of low-wavenumber vibrations. Of particular interest is a complicated feature at 400–450 cm^{-1}, which we assign to transitions between a number of vibrational and vibtor levels, some of which are in Fermi resonance.

Other workers have previously studied the $S_1 \leftarrow S_0$ spectrum of *p*Xyl;[19,20,21,22,23,24,25,26,27] additionally, resonant absorption studies have been performed on the cation, combining REMPI spectroscopy with photoelectron spectroscopy (REMPI-PES)[22] as well as the higher-resolution techniques of ZEKE spectroscopy[28] and mass-analyzed threshold ionization (MATI) spectroscopy.[25,26,29] In addition to a HeI photoelectron spectrum that exhibited some partially-resolved but unassigned vibrational bands.[30,31,32,33] there has been an early photoionization study by Watanabe. [34] We shall refer to the previous studies at appropriate points in the present work.

We shall also compare the spectral activity observed to that discussed in our earlier work on pFT,[35,36] as well as the more-recent work on the latter molecule by the Lawrance group and ourselves.[37,38,39,] In addition, we shall comment in passing on previous work on pFT.[40,41,42] Additional comparisons will be made to earlier results on para-difluorobenzene (pDFB): for the $S_1 \leftarrow S_0$ transition, earlier key papers for pDFB have been published by Covaleskie and Parmenter[43] and Robey and Schlag,[44] amongst others, but these have been largely superseded by the thorough analysis of laser-induced fluorescence (LIF) and dispersed fluorescence (DF) spectra by Knight and Kable.[45] In addition, ZEKE spectra of pDFB have been published by Reiser et al.,[46,47] where a number of different intermediate S_1 vibrational states were employed.

II. EXPERIMENTAL

The vapour above room temperature para-xylene (99.5% purity, Sigma-Aldrich) was seeded in ~1.5 bar of Ar and the gaseous mixture passed through a General Valve pulsed nozzle (750 μm, 10 Hz, opening time of 180–210 μs) to create a free jet expansion.

The REMPI and ZEKE apparatus employed has been described previously in detail elsewhere,[48,49] and so only a brief description is required here. The excitation laser was a dye laser (Sirah Cobra-Stretch) operating with C540A and was pumped with the third harmonic (355 nm) of a Surelite III Nd:YAG laser. The ionization laser was a dye laser (Sirah Cobra-Stretch) operating with DCM. In the case of the ZEKE spectrum recorded via the S_1 origin, a mixture of Rhodamine B and Rhodamine 101 was used, in order to scan to higher energy. In each case, this laser was pumped with the second harmonic (532 nm) of a Surelite I Nd:YAG laser. The fundamental frequencies produced by each dye laser were frequency doubled using BBO and KDP crystals for the pump and probe lasers, respectively. The focused, frequency-doubled outputs of the two dye lasers were overlapped spatially and temporally and passed through a vacuum chamber coaxially and counterpropagating. Here, they intersected the free jet expansion between two biased electrical grids located in the extraction region of a time-of-flight mass spectrometer, which was employed in the REMPI experiments; these grids were also used in the ZEKE experiments by application of pulsed voltages, giving typical fields (F) of ~10 V cm^{-1}, after a delay of up to 2 μs, where this delay was minimized while avoiding the introduction of excess noise from the prompt electron signal.

Bands had widths of ~5-7 cm^{-1}, even when $\sqrt{F}$ relationships would suggest the widths should be significantly greater, because of the well-known decay of the lower-lying Rydberg states accessed in the pulsed-field ionization process.[50]

III. COMPUTATIONAL DETAILS

The geometry of each electronic state was optimized. For molecules such as toluene and pFT, two key geometries arise from the orientation of the methyl group with respect to the phenyl ring. If one of the methyl C–H bonds is in the same plane as the phenyl ring, this is called "eclipsed", while if one is perpendicular to the ring, this is called "staggered". In the case of pXyl, either of these may occur for each methyl group, which we term "eclipsed-eclipsed" and "staggered-staggered" but, further, it is possible for the two methyl groups to be eclipsed or staggered with respect to each other. For simplicity, we append "*cis*" or "*trans*" to the front of the eclipsed-eclipsed or staggered-staggered designation, respectively, to represent these. There are hence five main different conformers to consider: *cis*-eclipsed-eclipsed; *trans*-eclipsed-eclipsed; *cis*-staggered-staggered, *trans*-staggered-staggered; and staggered-eclipsed. We found that the lowest energy conformers for all three of the S_0, S_1 and D_0^+ states were staggered-staggered, but we find that the S_0 and D_0^+ states had lowest-energy conformers that are *trans*-staggered-staggered, while the S_1 state was calculated to have a *cis*-staggered-staggered global minimum. We obtained all real vibrational wavenumbers for the S_1 and D_0^+ structures, but still obtained an imaginary value for the S_0 state, with its form suggesting torsional movement; however, we did not pursue this further for two reasons. First, we note that the B3LYP/aug-cc-pVTZ methods employed herein are unlikely to give definitive results regarding the geometric parameters, since much of the torsional potential will be determined by van der Waals interactions between the methyl hydrogen atoms, and those closest ones in the phenyl ring (although other interpretations of methyl torsional potentials have been put forward). Secondly, the actual torsional potential parameters will be affected by vibrational zero-point energy for the different structures and so reliable values for these, noting that both vibrational anharmonic effects and vibrational-torsional interactions are likely to be necessary, are hard to obtain. Hence, it is likely to be exceedingly difficult to calculate reliable torsional potentials using quantum chemical methods;

particularly with the expected need for high-level methods to account for the weak interactions that give rise to the potential. It can be concluded from our calculations that the barriers are small (< 20 cm^{-1} and likely lower), and hence that only the very lowest torsional levels are likely to lie below the barriers.

As an aid to the assignment of our spectra, the vibrational frequencies of pXyl were calculated using the GAUSSIAN 09 software package[51] and are presented in Table I, where all of the calculations used default parameters. If the methyl groups are considered as point masses, then the pXyl molecule may be considered as belonging to the D_{2h} point group, and we shall see that much of the vibrational activity is understandable as such. For the S$_0$ ($\tilde{X}$ ^1A_g) ground electronic state, B3LYP/aug-cc-pVTZ calculations were employed; for the S$_1$ ($\tilde{A}$ $^1B_{2u}$) state TD-DFT, B3LYP/aug-cc-pVTZ calculations; and for the D$_0^+$ ($\tilde{X}$ $^2B_{1u}$) ground state cation, UB3LYP/aug-cc-pVTZ calculations, which yielded <S^2> values of ~ 0.76, indicating spin contamination was minimal. (The axis system employed will be noted later.)

As discussed in ref. 14, we label the S$_0$ vibrational modes by comparing the molecular vibrations with those of pDFB. This scheme, with vibrational labels D_i, has been designed to allow application both to symmetric and asymmetric $para$-disubstituted benzene molecules and is based on a Mulliken[17]/Herzberg[18] labelling of the vibrations of pDFB, but in the C_{2v} point group. This scheme gives a clear and unambiguous assignment of the vibrational modes which are localized to the phenyl ring and allows these to be mapped across a wide range of symmetrically and asymmetrically-substituted molecules. Also in that work,[14] we presented an analysis whereby the relationship between the D_i labels and the M_i labels[6] employed for monosubstituted benzenes was given. Since we shall occasionally need to refer to these two sets of labels in the present work, we report here the results of such a vibrational analysis for pXyl, where we follow the procedure described in ref. 14; namely, employing the calculated force field for pDFB, but with the methyl groups represented by F atoms with masses of 15 amu – the results are presented in Table II. Of note is that there are a number of D_i modes that do not correlate with any M_i mode and, as discussed in ref. 14, in many cases there is no clear match to any Wilson[15] mode either; this means that using such Wilson labels for these modes in the manner of Varsányi[16] is misleading. (The CH$_3$-localized vibrations are easily identified from the calculated vibrations and do not form part of the D_i labelling scheme.)

For the S_1 and D_0^+ states of pXyl, we find that the vibrational motions were often altered slightly from the S_0 motion, but it was always possible to identify the most appropriate D_i label in each case. These assignments will, however, not include any strong resonance effects, such as Fermi resonance (FR); in such cases, the actual eigenfunctions will correspond to mixtures of the D_i zero-order state (ZOS) motions. The calculated vibrational wavenumbers for the D_i modes are presented in Table I for both the S_1 and D_0^+ states of pXyl. In addition, we present similar results for pDFB and pFT, which we shall use later to compare the REMPI and ZEKE spectra of these molecules to those of pXyl. We note, however, that although there was no issue for the S_0 and D_0^+ states, the calculated wavenumber of the S_1 state D_{14} vibration is not viewed with any confidence since the corresponding M_{14} vibrational wavenumbers were deemed unreliable in our previous work on the monohalobenzenes.[54,55,56]

IV. Molecular Symmetry Group of pXyl and Its Torsional Levels

As discussed in our accompanying paper,[13] to consider the spectroscopy of pXyl involving the torsional levels requires consideration of the molecular symmetry. The molecular symmetry group (MSG) of pXyl may be designated $[3,3]D_{2h}$ which may be seen to be isomorphic with the G_{72} MSG, which has been discussed by Bunker and Jensen.[52] It proves more straightforward to use G_{72} labels in discussing the spectroscopy of pXyl, with the details of the MSG notation being given in ref. 13. The torsional levels of pXyl, may loosely be described as linear combinations of single-rotor levels of each methyl group, but there are different linear combinations for different levels each of which has a definite G_{72} symmetry – see ref. 13 for full details. The pXyl levels are designated $\{m_1, m_2\}$, but sometimes with an additional superscripted + or - to specify a particular linear combination; the m_1 and m_2 being the internal rotor quantum numbers of each methyl. Notably, it was shown that, although we are working under jet-cooled conditions, we expect to see four torsional levels populated owing to their having different nuclear spin symmetries: these are the $\{0,0\}$, $\{0,1\}$, $\{1,1\}$ and $\{1,-1\}$ levels, which we shall occasionally refer to as the "cold" $\{m_1, m_2\}$ levels. Because of the expected similarity in the torsional potentials in the three electronic states here, we find that, symmetry permitting, there will often be more than one transition associated with each REMPI or ZEKE band, arising from exciting within different torsional "ladders" associated with each of the cold $\{m_1, m_2\}$ levels. So, for example, the origin band and any band associated with a totally-symmetric vibration, will arise from four essentially degenerate (under our

resolution) transitions, one involving each of the cold $\{m_1, m_2\}$ levels. For simplicity, in most cases we shall not explicitly state all of the torsional levels involved; but, as will be seen, occasionally this is necessary to explain the observed features.

Further, it is expected that transitions involving various vibtor levels may be observed, either as a result of a transition to such a level or to levels that arise from FR between vibrational and vibtor levels. The reader may find it useful to refer to the character table and direct product table for the *p*Xyl MSG that have been presented in ref. 13.

V. RESULTS AND DISCUSSION

A. REMPI Spectrum - Overview

The 0–600 cm^{-1} region of the one-colour (1+1) REMPI spectrum of *p*Xyl is presented in Figure 1(a); in Figure 1(b) the corresponding spectrum of *p*FT is also presented – this has been discussed in detail in ref. 38; finally, in Figure 1(c), the two-colour (1+1') spectrum of *p*DFB is presented – the latter spectrum was recorded by our group recently and reported in ref. 38. The spectra are presented on a relative wavenumber scale, with the origin of the *p*Xyl spectrum found to be at 36724 ± 2 cm^{-1}. The latter value agrees well with the origin value reported by Selco and Carrick[53] (36725.3 cm^{-1}), which is in reasonable agreement with that determined by Blease et al. (36727 cm^{-1})[21] and Ebata et al. (36728 cm^{-1}).[19] However, other reported values have varied with 36732 cm^{-1} (ref. 20) and 36733 cm^{-1} (ref. 22) having been reported and even a value as high as 36738 cm^{-1} in refs. 25 and 26; the reasons for these discrepancies are not clear.

It is of note that much of the vibrational activity is the same across the three molecules (evident because of the same vibrational labelling scheme used), but that there is significantly more structure in the 0–300 cm^{-1} region for *p*Xyl and *p*FT than there is in the case of *p*DFB: this is due to the presence of the methyl group and hence torsional and vibration-torsional transitions, which are discussed in refs. 13 and 38, for *p*Xyl and *p*FT respectively.

In presenting and discussing the spectra of *p*Xyl, we label vibrational energy levels with the vibrational label, D_i; for vibtor levels, we specify both the vibration and torsional components.

We denote $S_1 \leftarrow S_0$ vibrational transitions in the usual way, and similarly for vibtor transitions. The notation for pDFB transitions clearly only involves vibrational quantum numbers and so is standard, while pFT transitions are labelled in an analogous manner to those of pXyl, but with changes in torsional quantum number only involving the single methyl group.

To specify the symmetry for benzene, toluene, pDFB and pXyl it is necessary to define the axis systems employed. For benzene, the molecule lies in the xy plane, with the z axis coincident with the C_6 symmetry axis. For a D_{2h} molecule, the z axis will pass through the fluorine atoms of pDFB, but the protocol for selecting the x and y axes are not so definitive. We follow the axis system employed by Knight and Kable,[45] who located the molecule, or more generally the phenyl ring, in the yz plane. A similar issue arises with a C_{2v} molecule and to be consistent with this and our previous work, we also locate the phenyl ring of the molecule in the yz plane, with the z axis passing through the unique substituent atom (or group) and the centre of the phenyl ring. With these axis conventions, in the D_{6h} point group for benzene, the S_1 state is designated $\tilde{A}^1B_{2u}$, the S_2 state is $\tilde{B}^1B_{1u}$, and the S_3 state is $\tilde{C}^1E_{1u}$. These will be pertinent to discussion of Herzberg-Teller (HT) vibronic coupling effects – see later.

Treating pXyl within the D_{2h} point group, the resulting transition may be denoted $\tilde{A}^1B_{2u} \leftarrow \tilde{X}^1A_g$; for molecules with C_{2v} point group symmetry, then the corresponding transition is $\tilde{A}^1B_2 \leftarrow \tilde{X}^1A_1$, and is the same transition observed in our recent REMPI work on monohalobenzenes[54,55,56] and in toluene,[2,3] and pFT[36,38,] (in the latter two cases, each methyl group is again taken to be a point mass). The correlations between the symmetries in the D_{6h} point group with those in the D_{2h} and C_{2v} ones, as well as those in the G_{12} and G_{72} MSGs has been presented in ref. 13.

The first ~ 300 cm^{-1} above the intense origin band of the spectrum of pXyl is shown in Fig. 1(a) and consists of mainly torsional bands (see ref. 13), while in the range 300–650 cm^{-1} there are a number of moderately-intense features that will be seen to be assignable to mainly vibrational bands, with the structured feature marked ξ arising from a series of transitions, some of which form part of a complex Fermi resonance, as we shall discuss. We note that some of the bands, including those that make up the feature labelled ξ, have been reported before,[19,21,22] although we shall not always agree with the assignments. In addition, we

comment on more of the observed features than has been done in those previous studies; in particular, we note that Ebata et al.[19] and Gunzer and Grotemeyer[25,26] assigned very few features in their wider-range spectrum and none below 650 cm^{-1}. In contrast, Blease et al.[21] gave assignments for four of the bands in this region, on which we shall comment below. The REMPI spectrum presented in ref. 25 appears to be the best quality of those previously reported (albeit with little comment on the assignment therein) and is in excellent agreement with that presented in Figure 1(a) of the present work. In the following, we shall discuss the assignment of the main REMPI features by reference both to our and others' previous pFT work, as well as to the activity we see in the ZEKE spectra when we excite through the various S$_1$ levels that are the terminating states of various REMPI transitions.

We have identified some bands in the spectra in Figure 1 that are attributable to complexation of the parent molecule with Ar. These are identifiable by: their changing relative intensities with expansion conditions; the observation of the parent cation in the mass spectrum; and, in the case here of pXyl, by comparison with the work of Lu et al.[57]

B. ZEKE spectrum via the origin

In Figure 2(a) we show the 0-600 cm^{-1} region of the ZEKE spectrum when exciting via the S$_1$ origin. Note that there is a general "$\Delta v = 0$" propensity rule for substituted benzenes whereby the most intense ZEKE bands correspond to the same vibration as the intermediate S$_1$ vibrational level. Hence, it is no surprise to see that the ZEKE spectrum is dominated by the intense origin band. From its position, we can determine the adiabatic ionization energy (AIE) of pXyl as 68200 ± 5 cm^{-1}, with the uncertainty arising from the width of the ZEKE bands and the uncertainty in the absolute wavenumber scale. This equates to 8.456 ± 0.001 eV, which agrees well with earlier determinations of this quantity, [30,31,32,33,34] albeit with significantly lower precision therein. When we compare to recent ZEKE and MATI values, we find good agreement with the MATI value of Gunzer and Grotemeyer (68204 ± 4 cm^{-1}),[26] but the value of Held et al.[28] (68186 ± 2 cm^{-1}) is somewhat too low.

 The assignment of the ZEKE bands in Fig 2(a) comes from their observation in other ZEKE spectra obtained via different intermediate levels, and those spectra will be discussed below, so only general comments will be made here. First, it is noteworthy that as well as the

transition to the origin, we also see significant bands arising from D_{19}, D_{14} and D_{11} cation levels. The main FC-allowed bands, apart from 11_0^1, are the $29_0^1 m_{\{0,0\}}^{\{0,3(+)\}^-}$ and 19_0^2 bands, recalling that we shall not specify torsional levels unless required (see above). In addition, close to the origin are a series of "pure" torsional and vibtor bands, which have been discussed elsewhere,[13] and some of these may be seen across the spectrum associated with vibrational bands. Of note is that we see a band that could be associated with the $\{0,3(-)\}^-$ level, which can be viewed as an analogue of the 3(-) level in a single-rotor system such as toluene or pFT. As discussed in ref. 38, we observed the 3(-) state when exciting via the origin for pFT, which is attributable to electronic-torsional coupling. We have discussed in ref. 13 the corresponding situation for pXyl.

Very weak bands are also seen in the origin ZEKE spectrum that we can assign to transitions to the D_{28} and D_{29} vibrational levels, which are both of b_{3g} symmetry; these appear to be active as a result of a small amount of vibronic coupling – their assignment will be confirmed later. As noted for pDFB,[47] and as will be revisited later in the present work, there appear to be mechanisms available to relax the usual vibrational symmetry selection rules in these species.

In Figs 2(b) and 2(c), we have also plotted the corresponding region of the ZEKE spectra for pFT and pDFB, each of which may be seen to show remarkably similar vibrational activity, albeit with intensity variations. The reader is referred to ref. 38 for a fuller discussion of the pFT assignments, while the ZEKE spectrum for pDFB has been constructed from the trace in ref. 47 and assignments have also been taken from there, but changing the vibrational labels to D_i ones; we also added the assignment of the D_{28} to this spectrum, as a band position agrees well with the calculated vibrational wavenumber.

Rather unexpected is the assignment by Zhang et al.[29] of the 340 cm^{-1} feature in the ZEKE spectrum of pXyl to a vibration associated with the ν_3 Wilson mode. Table II shows that ν_3 correlates best with the D_{26} vibration; however, this would be expected at around 1250 cm^{-1} in the MATI spectrum, so the assignment of ref. 29 must be incorrect; this misassignment seems to be attributable to the use of the Varsányi[16] labels. The band observed here at 341 cm^{-1} was also reported in ref. 25 and assigned there to cation Wilson mode ν_{16a}, which is

almost identical in form to D_{14} (see Table II and ref. 14). This fits well to both the calculated value – see Table I –and to the observed position of the (FC-allowed) overtone band, 14_0^2. Overall, we prefer the assignment of the 341 cm^{-1} band to 14_0^1 over an alternative one, $19_0^1 20_0^1$, since the latter is not symmetry allowed in D_{2h}; it would also be expected to be weak as it arises from two non-totally-symmetric contributions. In addition, a D_{14} band can be seen in the corresponding ZEKE spectra of pFT and pDFB in a relatively similar position, while the $19_0^1 20_0^1$ band would be expected at significantly different wavenumbers for these molecules (see Table I) and nonesuch is observed.

As mentioned, many of the cation levels accessed in this spectrum will also be observed via different intermediate levels, and the activity in those ZEKE spectra will be seen to differ dramatically from that in Figure 2(a). This shows the utility of using the two-colour ZEKE technique. Further comparison will also be made to the corresponding ZEKE spectra for pFT and pDFB later in the text.

C. ZEKE spectrum via D_{29}

The ZEKE spectrum recorded when exciting through the feature at 372 cm^{-1} is shown in Figure 3. (Excitation at this wavenumber corresponds to the cleanest spectrum, although the peak of the REMPI feature is actually at 370 cm^{-1}.) Since the ZEKE spectrum obtained when exciting via the 372 cm^{-1} S_1 level is dominated by a band at 378 cm^{-1}, which best fits the calculated value for D_{29}, then the $\Delta v = 0$ propensity rule identifies the S_1 intermediate level as D_{29}. We note that this vibration cannot be associated cleanly with any single Wilson mode (Table II). Since the intermediate level is a b_{3g} mode within the D_{2h} point group, we expect to see mainly bands associated with levels of such symmetry dominating the ZEKE spectrum. Indeed, the majority of the bands can be assigned to levels with this symmetry, also providing further confirmation of the assignment of the S_1 vibrational level. This vibration has been wrongly associated with Wilson mode ν_{9b} in previous work,[21,22,25,26,28] based on the erroneous assignment of this mode by Varsányi;[16] however, the ν_{9b} vibration is most similar to mode D_{23} and so is expected to be much higher in wavenumber.

To higher wavenumber we also see the $11_0^1 29_1^1$ combination band and various other weak features. We have made an attempt at assigning the latter based upon activity in other ZEKE spectra and calculated wavenumbers. Our best suggestions are given in Figure 3. Note that we observe a weak origin band, which is FC-forbidden and so must arise as a result of vibronic effects, noting that we also saw a weak D_{29} band in the ZEKE spectrum recorded when exciting via the origin. As a consequence, we are comfortable with the assignment of some other weak features to totally-symmetric (and hence symmetry forbidden in the present case) vibrations: we reiterate that the two strongest bands are assigned to FC-allowed vibrations. It is notable that we see the $\{0,3(+)\}^-$ torsion and the D_{11} $\{0,3(+)\}^-$ and D_9 $\{0,3(+)\}^-$ vibtor levels; these have the same MSG symmetry as the intermediate D_{29} level, namely a_4'' explaining their activity. It is also interesting to note that we see a band at 77 cm^{-1}, which is assignable to an $\{m_1,m_2\}$ level with $m_2 = 4$. This band must arise from vibtor contributions from the other cold torsional levels, $\{0,1\}$, $\{1,1\}$ and $\{1,-1\}$ each associated with the D_{29} level. As an example, the $\{0,1\}$ level has g'' symmetry and so the D_{29} $\{0,1\}$ level has g' symmetry, which is the same as the $\{0,4\}$ level indicating how the latter may appear; similar arguments suggest that in fact the 77 cm^{-1} band comprises two other transitions terminating in the $\{1,4\}^-$ and $\{1,-4\}^-$ levels (see ref. 13 for notation); these will be inseparable with our resolution.

In ref. 47, Reiser et al. reported a ZEKE spectrum of pDFB when exciting through the D_{29} vibration (designated as Mulliken mode 27 therein). They observed the same strong $\Delta v = 0$ band, plus the combination band with D_{11}. They also saw further overall b_{3g} symmetry combination bands when scanning to higher wavenumber than here. Interestingly, in pFT the 29_0^1 REMPI transition is overlapped with the 14_0^2 one, as could be ascertained from the behaviour of the ZEKE spectra, as discussed in ref. 36. These indicate that the major activity in the ZEKE spectrum when exciting at a wavenumber where the feature is dominated by the 29_0^1 part of the feature is to the $\Delta v = 0$ transition, together with the $11_0^1 29_0^1$ combination, consistent with pXyl here, and pDFB.[47]

It is worth highlighting that we see combination bands of the $\Delta v = 0$ feature with D_{19}, D_{14} as well as D_{11} in the spectrum – the frequent appearance of this trio of combinations was highlighted in our work on pFT[38] where the signal-to-noise allowed us to see these in many cases. The appearance of these bands is believed to be due to various vibronic coupling mechanisms, although a complete mechanism has not been established. [38,47]

D. ZEKE Spectrum via D_{28}

We shall come back to the complicated feature ξ at 400 – 450 cm^{-1} – see Figure 1(a) – in the next subsection and will first consider the ZEKE spectrum obtained when exciting through the level corresponding to the higher-wavenumber REMPI feature at 554 cm^{-1}; this ZEKE spectrum is shown in Figure 4. The very strong ZEKE band at 555 cm^{-1} is at a very similar wavenumber to the intermediate level and so is consistent with the ZEKE band being assigned to D_{28} with the intermediate level therefore being the corresponding S$_1$ state vibration, based upon the calculated wavenumbers in Table I and the $\Delta v = 0$ propensity rule. This vibration may be closely associated with the ν_{6b} Wilson mode (Table II) and so agrees with the previous assignment in ref. 22, as well as the assignment of the intermediate level by Blease et al.[21] Consistent with the ZEKE spectrum via the D_{29} intermediate level, here we also observe the $11_0^1 28_0^1$ combination band to higher wavenumber as well as a number of other weaker features. Our suggested assignments for the latter are given in Figure 4; note that the majority of these have the same symmetry as the D_{28} vibration, namely b_{3g} under D_{2h} symmetry. (Unfortunately, owing to technical issues, we did not scan to low enough wavenumber to see features such as the origin and {0,3(+)}$^-$ bands, which were seen when exciting via the S$_1$ D_{29} level; but we would have expected to observe these, since the symmetries of the D_{28} and D_{29} vibrations are the same.)

In passing, we note that Gunzer and Grotemeyer[26] have reported a MATI spectrum of pXyl via this level, but only a very limited region of the spectrum was reported, mainly showing the $\Delta v = 0$ band; no assignment was offered for this feature. No ZEKE spectrum for pDFB was recorded via the D_{28} (Mulliken mode 26, analogous to Wilson mode 6b – see Tables I and II) in ref. 47. The corresponding spectrum was reported by ourselves previously for pFT,[36] (noted therein as excitation of the Varsányi mode ν_{6b} at 549 cm^{-1}) and the present spectrum is very similar to that.

Again, we note that we see the vibronically-induced combination bands of the $\Delta v = 0$ feature with D_{19}, D_{14} as well as D_{11} in the spectrum, as we do when exciting via the origin and D_{29}.

E. Feature ξ at 400–450 cm^{-1}

We now move onto the complicated feature ξ in the S$_1$ ← S$_0$ REMPI spectrum of pXyl – see Figure 1(a). This appears in the range 400–450 cm^{-1} and is shown in an expanded form in Figure 5. It appears to consist of at least three main bands, which we label ξ_A, ξ_B and ξ_C with two weaker features to lower wavenumber. This feature is reminiscent of a Fermi resonance (FR) seen in toluene that appears in the range 440–470 cm^{-1}, which has been examined in detail by 2D-LIF,[7] tr-PES[8] and by ZEKE spectroscopy;[2] there are also similarities to a feature observed in the range 395-415 cm^{-1} in pFT.[36,37,38] For toluene, the complex Fermi resonance was found to consist of three contributions: M_{11}, $2M_{14}$ and $M_{19}M_{20}$. From Table II we see that the M_{11} mode closely corresponds to D_{11}, and M_{14} is very closely aligned with D_{14}. Similarly, the major contributors to the corresponding feature in pFT are $2D_{14}$ and D_{11} (although the 29_0^1 transition actually overlaps the 14_0^2 one in pFT, but these are of different symmetries and are not thought to be interacting); there is also evidence for the involvement of the D_{14} m = 6(-) vibtor level. [36,37,38] The calculated wavenumbers for both $2D_{14}$ and D_{11} suggest that the corresponding transitions should be at approximately the same position in pXyl, and so may be expected to contribute to this region. The involvement of the equivalent of the $M_{19}M_{20}$ combination does not need to be considered here for two reasons: first, D_{19} and D_{20} have different symmetries in the D_{2h} point group, despite being of the same symmetry under C_{2v} symmetry (interestingly both contain dominant contributions from M_{20}, see Table II) and so their combined symmetry is not totally symmetric; and secondly, the calculated wavenumber for the $D_{19}D_{20}$ combination in the S$_1$ state is $\sim$ 310 cm^{-1} in pXyl – far away from the D_{11} and the D_{14} overtone vibrations, and is not seen here. Hence, we anticipate the ZEKE spectra to concur with two of the previous toluene and pFT assignments, but we shall require at least a third contribution to feature ξ, with the possibility of other contributions to this spectral range.

We note that the present feature ξ was identified only as a single band at 424 cm^{-1} in ref. 22 and assigned to Wilson mode ν_{6a}, which corresponds closely to D_{11} (which in turn correlates closely to M_{11} for toluene). In ref. 25, a band at 440 cm^{-1} was reported, but was not assigned. On the other hand, the slightly earlier paper of Blease et al.[21] identifies two contributions (at 425 and 433 cm^{-1}), which they assign to the ν_{6a} fundamental and the ν_{16a} overtone, using Wilson notation; as will be seen, we concur to some extent with these two assignments

(relabelling the vibrations as D_{11} and $2D_{14}$), but we shall conclude these are not the only contributions to this region and that D_{11} is to lower wavenumber.

In Figure 6 we show a series of ZEKE spectra recorded at excitation wavenumbers within the bands that make up feature ξ. We have recorded more spectra than this at various positions and, taken together, we term this a "two-dimensional ZEKE" ("2D-ZEKE") spectrum; here we have selected those individual spectra that most clearly show the different ZEKE bands we observe. The positions at which these spectra were recorded are indicated on an expanded section of the REMPI spectrum, presented as a vertical trace on the right-hand side of Figure 6, with the ZEKE spectra being linked to these by dashed lines. As may be seen, these excitation positions do not always correspond to the peaks of the bands: the positions at which the clearest ZEKE features arise are likely a combination of a maximizing of the contribution of one component band to the feature over others, together with the portion of the rotational manifold that is excited within the laser bandwidth. In Figure 6 is the ZEKE spectrum recorded via the origin, and then the series of spectra follow in order of the intermediate excitation wavenumber. Although there are three easily identifiable substructures within feature ξ (see Fig. 5 and the right-hand vertical spectrum in Figure 6), each of these could arise from more than one overlapping band and hence be associated with more than one eigenstate; additionally, each contributing eigenstate could be composed of more than one ZOS as the result of Fermi resonance.

The 2D-ZEKE spectrum contained in Figures 6(b)–(i) shows that different features appear with differing intensities as we move across the wavenumbers corresponding to the bands shown in the accompanying $S_1 \leftarrow S_0$ spectrum (vertical trace). We attribute this behaviour to overlapped features in the REMPI spectrum: as we excite via different positions, we excite greater or lesser proportions of the various eigenstates. These eigenstates, and their ZOS make-up, in principle can be deduced from the activity seen in the ZEKE spectrum. In assigning these spectra we make use of the calculated vibrational wavenumbers presented in Table I, but give more weight to what are expected to be the more reliable cation vibrational wavenumbers over those of the S_1 state.

The assignment of the ZEKE spectra recorded via feature ξ_A caused particular difficulty. First, previous work on toluene and pFT, plus more directly the work on pXyl by Blease et al.[21]

suggest that the D_{11} vibration may contribute to this region, and indeed a weak band is observed at 439 cm^{-1} in the ZEKE spectrum when exciting at 424–428 cm^{-1} – see Figures 5(b) – (e). It is clear that neither of the two more-intense contributions to the ZEKE spectra, traces (b)–(e), are in the correct position and so any contribution from D_{11} to the REMPI spectrum in this region would be, at best, small. A careful examination of the relative band intensity of the 439 cm^{-1} feature compared to other bands around does not lead to a definitive conclusion about its behaviour as it is overlapped by the 427 cm^{-1} band. The band is fairly weak, although some caution is required since D_{11} could have a low photoionization cross section, as was the case for M_{11} in toluene;[2] however, its intensity via the origin and the relative intensities of other bands does seem to suggest its contribution is small to this region. We further note that the calculated and experimental values for D_{11} in the S_1 state are in good agreement for toluene and pFT, suggesting the same would be true for pXyl. This would suggest a value for the D_{11} vibration in the S_1 state of 400–405 cm^{-1}, which is good agreement with a weak feature at 404 cm^{-1} in the REMPI spectrum (see Figure 5); unfortunately, no ZEKE spectrum was recorded via this feature, nor for the other weak band at 414 cm^{-1}, which may be assignable to the 20_0^4 transition. We note, however, that with the uncertainty in the calculated values and with anharmonicity, the assignments of the 404 and 414 cm^{-1} features could be reversed. In line, therefore, with some other substituted benzenes, such as fluorobenzene[54,58,59] the M_{11}/ D_{11} vibration appears to be very weak in the present case. The differing intensity of this vibration in $S_1 \leftarrow S_0$ transitions of substituted benzenes could be attributable to Herzberg-Teller vibronic coupling as discussed by Blease et al.[21] and as we commented on for pFT.[38] Thus, we conclude that the majority of the intensity of feature ξ_A comes from other vibrations.

To assign the other contributions to this feature, we initially note that the two "humps" on the higher wavenumber side of band ξ_A resemble closely the profile of band ξ_B, which we show below appears only to have a single contributing eigenstate. Hence, we conclude that a similar envelope is associated with an eigenstate that gives rise to the blue side of band ξ_A. This is supported by the very similar appearance of the two ZEKE spectra recorded at 427 and 428 cm^{-1}, and suggests that the two intense ZEKE bands observed arise from a single eigenstate that is composed of significant contributions from two ZOSs. Further, since the same two bands appear in the ZEKE spectrum recorded when exciting through the red side of

feature ξ_A, we suggest that there are two S_1 eigenstates that lead to intensity in feature ξ_A: one eigenstate is the majority contributor to the blue edge of feature ξ_A, while the other eigenstate mainly contributes to the red side, but the two contributions overlap in the centre – see Figure 7 for a schematic representation of this, where we have assumed that each transition gives rise to similar band profiles.

We also find that the band at 470 cm^{-1} is the most intense in all ZEKE spectra when exciting across feature ξ_A, even though the relative intensities of other features are changing; this suggests that one of the ZOSs has a significantly higher photoionization cross section than the others. The other key ZEKE bands are the ones at 426 and 547 cm^{-1}. The 426 cm^{-1} band has its largest relative intensity compared to the 470 cm^{-1} band when exciting at 428 cm^{-1}. The weak contribution from the D_{11} vibration to the ZEKE spectrum may simply be FC activity, but could also indicate weak coupling of this vibration to the other ZOSs in this region – tr-PES results would be useful to gain further insight into this point.

Various other contributing ZOSs were considered, and we briefly discuss a few before providing our favoured assignment. The $D_{19}D_{20}{}^2$ transition is expected at about this position in the S_1 state and the cation values are also in about the correct position. However, this transition would be expected to be weak and hence we would need another interacting partner for a Fermi resonance; the D_{18} vibration would appear to match the REMPI and ZEKE band positions well and so might have been a contender. However, we eventually excluded these since, although these two vibrations have the same symmetry under C_{2v} symmetry, we find that D_{2h} selection rules appear to hold well for pXyl and the D_{18} and D_{19} vibrations have different symmetry in the D_{2h} point group; hence these levels would then not be expected to interact. Another possible contributor would be $4D_{20}$, which is expected to the low side of the REMPI feature as noted above. In the cation, the frequency is expected to be ~ 400 cm^{-1} and thus too low for the main ZEKE bands for this to be a viable contender for these. However, we note that there is a weak ZEKE band at 385 cm^{-1} seen when exciting at 424 cm^{-1} and, although this could be assignable to D_{29} this is symmetry forbidden and only a very weak D_{29} band was seen when exciting via the intense origin, but this could arise as a $\Delta\{m_1,m_2\} = -3$ band, but the intensity of the "parent" vibtor band (see below) suggests this is unlikely. We currently tentatively assign this band as a transition to $4D_{20}$, which suggests that there may be some weak interaction between this vibration and the other levels that contribute to the

more intense bands in feature ξ: as noted above, a weak band attributable to a transition to $4D_{20}$ is seen in the REMPI spectrum at ~ 414 cm^{-1}. (We note in passing that the M_{20}^4 overtone was assigned in the REMPI spectrum of chlorobenzene.[55])

After examining the various other possibilities for the main ZOS contributors to these regions of the REMPI and ZEKE spectra, we have concluded that the most likely additional contributors to feature ξ_A are the D_{19} overtone transition, 19_0^2 and the vibtor transition, $29_0^1 m_{(0,0)}^{\{0,3(+)\}^-}$. Both of these states are totally symmetric overall and hence could interact with each other. We highlight that the unperturbed $2D_{19}$ and D_{29} m = {0,3(+)}$^-$ ZOSs are expected to be at about the same wavenumber (within experimental and calculational uncertainty) in the S$_1$ state and after interaction, the resulting eigenstates appear to be separated by ~ 10 cm^{-1}. Since we saw no clear evidence for a transition to D_{29} {0,3(+)}$^-$ in the ZEKE spectra of pFT,[38] this suggests that it is not intrinsically bright. Together with the observation of a bright $2D_{19}$ band in pFT[38] , this allows us to assign the more intense band at 470 cm^{-1} to the 19^2 ZEKE band. Additionally, we note that in the present case, both of the ZEKE features at 426 and 470 cm^{-1} are seen distinctly when exciting via the origin, see Figure 2(a) and Figure 6(a), but are considerably weaker than the D_{11} band, suggesting the intensity of the latter is mainly associated with activity during the D$_0^+$ $\leftarrow$ S$_1$ 0^0 ionization. We thus conclude there are two eigenstates that are the main contributors to feature ξ_A, each made up of significant contributions of each of the (bright) $2D_{19}$ and (dark) D_{29} m = {0,3(+)}$^-$ ZOSs, with each eigenstate having a majority contribution from one of these. The D_{19} overtone appears to be the majority contributor to the lower wavenumber S$_1$ eigenstate (since the 470 cm^{-1} ZEKE band has its greatest relative intensity when exciting at 424 and 426 cm^{-1}), while the D_{29} m = {0,3(+)}$^-$ ZOS is the majority contributor to the higher-wavenumber S$_1$ eigenstate (since the 426 cm^{-1} ZEKE band has its greatest relative intensity when exciting at 427 and 428 cm^{-1}). These statements take into account that the ZEKE band intensities must be affected by a higher photoionization cross section for the D_{19} overtone ZOS.

Lastly, we note that we observe a ZEKE feature at 548 cm^{-1} only when exciting on the low-wavenumber side of feature ξ_A – see Figures 6(b) and (c). Although this value is quite close to the value for the D_{28} cation vibrational wavenumber discussed above, it is far enough removed to suggest it is likely something else. Further, there is no obvious reason why there

should be activity in this mode when exciting through totally-symmetric vibrations – even when exciting through the intense origin, the vibronically-induced D_{28} is very weak in the ZEKE spectrum – see Figure 2(a). We thus sought another totally-symmetric assignment for this feature and, based on our work on pFT, we considered the D_{14} {0,6(-)}$^+$ vibtor level, which is totally symmetric. This level would be expected to have an S$_1$ wavenumber of about 420 cm^{-1} and a cation value of about 540 cm^{-1}, based upon expected wavenumber values for D_{14} and {0,6(-)}$^+$. Thus, it is reasonable to expect a contribution from D_{14} {0,6(-)}$^+$ to the low wavenumber side of the REMPI feature ξ_A in Figure 5, and a ZEKE band at 548 cm^{-1}, bearing in mind this could be interacting with other levels in the cation, such as 2D_{19} and hence be pushed up slightly in wavenumber. A firm assignment to the ZEKE band at 595 cm^{-1} has not been established, but one reasonable possibility would be 2D_{30} as a result of Franck-Condon activity.

The second REMPI feature in this region, ξ_B, has previously been associated with the D_{14} overtone ($\nu_{16a}{}^2$ in Wilson/Varsányi notation).[21] We present three ZEKE spectra recorded across this feature, which are all dominated by a ZEKE band at 683 cm^{-1}, which is in reasonable agreement with the expected position of 2D_{14} for the cation, based on the calculated value of the fundamental and a weak band at the same position that appears when exciting via the origin (Figure 6(a), and also see above). That the three ZEKE spectra in traces 6(f–h) look so similar suggests that all of the structure in feature ξ_B actually arises from partially-resolved rotational band envelopes largely associated with a single transition, 14_0^2.

Since the D_{14} overtone is totally symmetric and since it also is in close energetic proximity to the bands that make up feature ξ_A, then the various ZOSs could be in Fermi resonance. We note that in toluene the M_{11} and $M_{14}{}^2$ vibrations were in close proximity[2] and have been shown to be in weak Fermi resonance.[2,7,8] and a similar conclusion was reached for pFT.[38] It is therefore satisfying to note that there are indeed weak features in the ZEKE spectra which correspond to those seen in the ZEKE spectrum when exciting via different positions in ξ_A and, additionally, a weak feature attributable to 2D_{14} may be seen when exciting via those positions (see Figure 6). Thus, we conclude that in the S$_1$ state, the D_{14} overtone is in weak Fermi resonance with the eigenstates that make up feature ξ_A (noting that the D_{11}

contribution is minimal for *p*Xyl), but that it is inherently a bright ZOS; again, very similar conclusions as were reached in the case of *p*FT.[38]

In Figure 8, we show the $\Delta(v,m) = 0$ region when exciting at a wavenumber corresponding to the centre of feature ξ_A as well as the same region (i.e. not the $\Delta(v,m) = 0$ region) when exciting through the centre of feature ξ_B. It may be noted that the $2D_{19}$ ZEKE band appears in both cases as does the D_{11} band; however, the band associated with D_{29} $\{0,3(+)\}^-$ is essentially absent when exciting via the centre of ξ_B. Additionally, the band associated with $2D_{19}$ is significantly reduced in relative intensity when exciting via the eigenstate that is dominated by $2D_{14}$, while the D_{11} band is relatively enhanced. We conclude that there is either a greater FC overlap between the D_{11} and $2D_{14}$ levels than between $2D_{19}$ and $2D_{14}$ ones, or possibly that the D_{11} and $2D_{14}$ are coupled more strongly than are D_{11} and $2D_{19}$; time-resolved results would be useful in untangling this, although energetic proximity and the weak intensities of the D_{11} bands suggests that FC overlap is the more likely explanation. Additionally, we note that a weak band appears when exciting through the $2D_{14}$-overtone-dominated level (see Figure 8), and this is assignable as a transition to $D_{14}D_{20}$ in the cation.

Finally, we consider the weaker band to higher wavenumber in the REMPI spectrum, labelled ξ_C. Exciting at a wavenumber (440 cm^{-1}) corresponding to this feature gives rise to a single ZEKE band at 521 cm^{-1} –see Fig. 6(i). Since we were unable to identify any other pure vibrational fundamental, overtone or combination band as a reasonable assignment for this feature, we searched for a vibtor assignment. An assignment of this band as being due to the D_{18} $\{0,3(-)\}^-$ vibtor level in the cation fits the position of the ZEKE band reasonably well,[28] yielding a value for D_{18} in the cation as 476 cm^{-1}, in good agreement with the calculated value. Assuming the $\Delta(v,m) = 0$ propensity rule, this then suggests a wavenumber of around 400 cm^{-1} for D_{18} in the S_1 state, which is somewhat below the calculated value; however, we note that a similar discrepancy arises for the D_{18} vibration in *p*DFB where the calculated S_1 value (Table I) is about 50 cm^{-1} higher than the assigned value from ref. 45. Assuming the calculated S_1 value is in error by a similar amount, and on the basis of the good agreement with the cationic values, we assign feature ξ_C in the REMPI spectrum to D_{18} $\{0,3(-)\}^-$. It is interesting to note that we observed a related feature in toluene close to this position that we assigned to

M_{18} m = 3(-), but we note that the D_{18} vibration more closely resembles M_{19} (see Table II and ref. 14) so this correspondence seems to be coincidental.

There are a number of other weak features present in the ZEKE spectra, but their assignment is not always definitive. We have hence provided our best assignments for these where possible, based upon: calculated vibrational wavenumbers; knowledge of the torsional energy levels and expected symmetry constraints; a_g symmetries being favoured throughout; b_{3g} symmetries being likely candidates in the S_1 state (via HT vibronic coupling); combination bands involving the D_{14} and D_{19} also appearing to be prevalent in the cation (see below); and then simply on energetic grounds thereafter.

In the next section, as part of an overview of the spectroscopy of disubstituted benzenes, we shall discuss the spectral activity seen for pXyl in relation to that seen for pFT and pDFB.

VI. FURTHER DISCUSSION

A. Overview of REMPI Spectra of pXyl, pFT and pDFB

REMPI spectra are given in Figure 1 for the three molecules of interest, with the vibrational assignments of the spectra of pFT[38,36] and pDFB[45] being based on previous work, but now employing the D_i labels. The 0–300 cm^{-1} regions of the spectra of pFT and pXyl (as well as toluene) have been compared in depth in ref. 13, where striking similarities for pFT and pXyl were seen up to 200 cm^{-1}. In the present work we shall only very briefly consider the low wavenumber region before moving to the higher wavenumber region.

It may be seen from Figure 1 that there is very little activity in the REMPI spectrum of pDFB in this wavenumber region, with only the origin and the 20_0^2 band being observed. In contrast, this region of the spectrum has a wealth of activity for both pFT and pXyl. As noted above, and based on the work on toluene in ref. 10, this arises from torsional levels and vibration-torsional levels and, as discussed in more detail for pFT in refs.37, 38 and 39 there are interactions between some of these levels. As a consequence, similar assignments are expected for pXyl, but complicated by the presence of two rotors – see ref. 13 for a fuller discussion and assignment of this region.

One other interesting aspect of this region of the spectrum is that the 30_0^1 transition is observed for pFT (albeit coincident with the $14_0^1 20_0^1$ transition)[37,38] , but not for pDFB nor

*p*Xyl. We attribute this to the fact that the D_{30} vibration is of b_{2u} symmetry in a D_{2h} molecule and hence not of the correct symmetry to be induced by Herzberg-Teller vibronic coupling, while the D_{30} vibration in *p*FT is of b_2 symmetry, and so now is vibronically-allowed, and hence observed. However, the $D_{14}D_{20}$ level is observed in all three molecules; this is of b_2 symmetry in *p*FT, and is of b_{3g} symmetry in D_{2h}, so is of the correct symmetry to be observed by Herzberg-Teller vibronic coupling in both cases. Above 350 cm^{-1}, we note that we observe the 14_0^2 transition for all of the molecules, with this being relatively separated in wavenumber in *p*DFB from any other vibration, confirming that the ZOS carries its own intensity; however, as we have noted above, there does seem to be some weak interaction between this overtone vibration and other vibrations within the complex FR feature at ~425 cm^{-1} in *p*Xyl and similarly for *p*FT. The appearance of the D_{29} {0,3(+)}$^-$ vibration within the FR for *p*Xyl seems to be as a result of its wavenumber being coincidentally close to that of the D_{19} overtone, and thus able to steal intensity from it. This conclusion is reached since the D_{29} vibration is to lower wavenumber in *p*Xyl than in *p*FT (and no evidence is seen of a band attributable to D_{29} $m =$ 3(+) in *p*FT, where it would be reasonably separated from other vibrations). Further, we note that separate features due to the 19_0^2 transition are also seen in *p*FT and *p*DFB, and so again we conclude that the ZOS carries its own intensity, consistent with our deductions above with regard to its role in the FR feature (ξ) for *p*Xyl. Finally, we have noted the appearance of a vibtor transition, $18_0^1 \, {}^{\{0,3(-)\}^-}_{(0,0)}$, which is reminiscent of a similar transition in toluene,[2] but we have noted the change in character between the monosubstituted benzene M_i modes, and the D_i modes of the disubstituted molecules (see above, Table II and ref. 14). However, the equivalent of this vibtor level does not appear in *p*FT (and, of course, cannot appear in the case of *p*DFB); hence, it does seem that there is a mechanism whereby this vibtor transition gains intensity in *p*Xyl, likely from the D_{14} overtone vibration, although such coupling is not evident from the ZEKE spectra. Finally, we note the appearance of the Herzberg-Teller induced D_{28} and D_{29} vibrations in the $S_1 \leftarrow S_0$ transition of all three molecules.

In summary, the above discussion supports the fact that the vibrational activity as a result of electronic excitation is very similar for these three molecules; something that is only clearly evident with a consistent labelling of the vibrations of these molecules.

There are other interesting aspects of the ~400 cm^{-1} FR region. First we note that in toluene, the M_{11} vibration was determined to be the bright state in the FR, with the $M_{19}M_{20}$ combination stealing intensity from it, and concluded to be dark, as was M_{14} overtone (refs. 8 and 9). As noted above, the intensities of the ZEKE bands for pXyl suggest that the D_{14} overtone is bright in the S_1 state, and indeed there is some evidence of this also for the M_{14} overtone in toluene.[2] Also, here we find that in pXyl the D_{11} band is extremely weak in the REMPI spectrum, and is also weak in the ZEKE spectra recorded when exciting across the wavenumber range of the FR. (We also noted that in toluene it seems that the M_{11} vibration has a low photoionization cross section, since the corresponding band is never the most intense feature.[2]) In fluorobenzene, the M_{11} band is also extremely weak in the $S_1 \leftarrow S_0$ transition,[54,58,59] and this has been associated with a small geometry change along that coordinate,[59] but the D_{11} bands for pDFB and pFT are reasonably intense.[45] Indeed, there is great variation in the intensities of the equivalent of the M_{11}/D_{11} band across substituted benzenes – perhaps more than one may expect for such similar molecules.[2,21,54,55,56] This point has been noted by Blease et al.[21] who concluded, on the grounds that there was very different one- and two-photon intensities of this band in their REMPI spectra, that in pXyl this mode gained intensity largely from HT intensity borrowing rather than via FC activity; they also remarked that the different relative vibrational intensities in different molecules may arise from the changing relative energies of electronic states (which may be viewed as being more likely to be changing significantly with substituent change than the ring geometry). Although we have concluded that there is only a minor contribution from D_{11} in the pXyl REMPI spectrum, we concur with the sentiments of Blease et al.[21] in that, although it is not entirely clear, it seems that the band they are referring to (the band assigned here to the D_{19} overtone band, but which they assigned as the v_{6a} (D_{11}) vibration) is very weak in their (2+2) REMPI spectrum. There is also similar evidence from one- and two-photon REMPI studies of the related molecule phenylsilane[60] where again some FC-allowed a_1 symmetry vibrations have very different intensities in the two spectra. In summary, we agree that some consideration ought to be given to HT activity affecting the intensities of vibrational bands involving a_g modes in pXyl, as well as those involving b_{3g} ones.

B. Overview of ZEKE Spectra

In Figure 2 we show the 0–600 cm^{-1} ZEKE spectra for the three molecules under discussion, in all cases recorded using the S$_1$ origin as the intermediate level. As is evident, and as with the REMPI spectra just discussed, with consistent labelling via the D_i labels the spectral activity can be seen to be very similar across this series of disubstituted molecules, even with shifts in wavenumber of the vibrations and some differences in relative intensity. For the vibrations in particular, the expected strong origin and also common D_{11} band is seen in all cases. We note that a band attributable to $2D_{19}$ appears in the spectrum of pXyl, but not in the spectra of pFT or pDFB. One explanation is that this may be attributable to the proximity of $2D_{19}$ to the D_{11} vibration in the cation in pXyl, and hence FR allows the D_{19} overtone to steal intensity from the D_{11} fundamental. Alternatively, since the $2D_{19}$ band is weak, it is not possible to rule out an explanation based on weak FC activity. Both of these explanations could be consistent with the observation of weak D_{11} bands when exciting via positions within feature ξ.

We note that in line with the Franck-Condon (FC) principle, we mainly expect to see totally-symmetric vibrations excited in the S$_1$ ← S$_0$ transition, since we are operating under jet-cooled conditions, and hence are exciting almost exclusively from the zero-point vibrational level. However, it is well-known that a number of non-totally symmetric vibrations appear in the electronic spectra of substituted benzenes, arising from HT interactions. (For the following discussion, the reader is referred to ref. 13, where correlations between symmetries in these point groups are exhibited.) For monosubstituted benzenes, such as the halobenzenes[54,55,56] and toluene,[2,3] these vibrations are of b_2 symmetry and are one component of the (analogue of the) e_{2g} vibration that allows the lowest $\tilde{A}\,^1B_{2u} \leftarrow \tilde{X}^1A_{1g}$ transition in benzene to be observed. The mechanism arises from a vibrational dependence of the transition dipole moment and may also be thought of as intensity stealing by the optically-dark S$_1$ state from the optically bright S$_3$ state in benzene, which is the $\tilde{C}^1E_{1u}$ state.[61,62] In D_{2h} symmetry, the S$_1$ ($\tilde{A}\,^1B_{2u}$) ← S$_0$ ($\tilde{X}^1A_g$) transition is now formally-allowed, but the vibronic interaction still exists and leads to the appearance of b_{3g} symmetry vibrations.[45] We note that the optically-dark S$_2$ ($\tilde{B}^1B_{1u}$) state of benzene becomes an optically-allowed $^1B_{1u}$ state in a D_{2h} molecule and so may also be partially responsible for some of the intensity of the b_{3g} vibrations. In addition, the other component of the D_{6h} $\tilde{C}^1E_{1u}$ state correlates with a $^1B_{2u}$ state under the D_{2h} point group

symmetry and this could also lead to HT activity in a_g vibrational modes under D_{2h} symmetry; this activity would be in addition to the FC-allowed activity of such modes.[21,62] It is not always straightforward to discern which mechanism operates, but as highlighted above in the case of pXyl, Blease et al.[21] have noted that differing one- and two-photon absorption spectra intensities for totally-symmetric modes indicate that HT mechanisms play a role for such vibrations.

At this point we note an interesting aspect of the ZEKE spectrum of pDFB:[47] to low wavenumber a number of sizeable FC-forbidden bands appear, which were assigned to the equivalents of D_{14}, D_{19} and D_{20}, which have respective symmetries, a_u, b_{2g} and b_{3u} (see Table I); additionally, combination bands involving the D_{14} and D_{19} vibrations were also reported for pFT,[38,36] both as fundamentals and in various combinations; these vibrations have respective symmetries a_2 and b_1 (see Table I). In the present pXyl ZEKE spectrum via the origin – Figure 3(a) – we also assign bands to the D_{14} and D_{19} vibrations and this indicates that similar mechanisms for their appearance operate in the pDFB and pXyl molecules. As with toluene[2] and pFT,[38,36] the D_{20} band does appear in the spectrum, but is heavily involved in vibration-torsion coupling – see ref. 13. However, the discussions for pDFB in ref. 45 regarding the LIF and DF spectra, and in ref. 47 regarding ZEKE spectra show that the precise mechanism is not well understood, and the present spectra do not appear to clarify the situation. We have discussed this a little further in our recent work on pFT,[38] where we suggest some possible perturbations to the force field may exist in the S_1 state, which may be giving rise to the forbidden D_{14} band in the ZEKE spectrum (and also explain the difficulty in calculating reliable D_{14} and M_{14} vibrational wavenumbers in the S_1 state of many substituted benzenes). The symmetry-forbidden D_{19} vibration can arise by HT coupling involving the D_0^+ and D_1^+ cationic states.

Another aspect of the vibrations of the disubstituted benzene cations is notable: the wavenumber of D_{11} is almost constant at ~440 cm^{-1} (see Table I), but in toluene it is somewhat higher at 496 cm^{-1} (ref. 2). Interestingly, the wavenumber of M_{11} in fluorobenzene is at a very similar value of 501 cm^{-1} (refs. 54,58,59), with the mass of F and CH$_3$ being very similar; while in chlorobenzene[63] the value has dropped to 422 cm^{-1}, because of the significantly heaver mass of the Cl atom.

VII. CONCLUDING REMARKS

We have investigated the lowest 0-600 cm^{-1} region of the S$_1$ ← S$_0$ REMPI spectrum of pXyl in detail. The investigation is via the activity we see in ZEKE spectra recorded via various S$_1$ intermediate levels; the assignment of the cation vibrations is based largely on the known torsional and vibration-torsional activity in toluene and pFT, and also on the calculated cation vibrational wavenumbers, with some consideration also being given to the calculated S$_1$ vibrational wavenumbers.

The ZEKE spectrum via the origin has been shown up to 600 cm^{-1} and shows strong activity in a_g modes, as expected; although some symmetry forbidden bands were also seen, in line with observations on the related pDFB molecule. Our assignment of the pXyl REMPI and ZEKE spectra differs markedly from the previous assignments, which suggested strong activity in symmetry forbidden modes; our reassignment is much more in line with observations on other substituted benzene molecules where the main activity in the photoionization step is from FC-allowed vibrational transitions, and so determined by the symmetry of the intermediate level. The low-wavenumber region of the REMPI spectrum has been found to consist of both torsional and vibration-torsional (vibtor) levels, and is discussed in the accompanying paper.[13]

We have identified two b_{3g} symmetry vibrations, D_{28} and D_{29} that are not strongly coupled to any other vibrations but which are evidence for the largely expected activity in b_{3g} modes in the REMPI spectrum, consistent with HT coupling. When exciting via these levels, we find activity mostly from b_{3g} levels in the ZEKE spectrum in line with the FC principle. We do, however, see indications of bands that are formally symmetry forbidden, including the origin, when exciting via these.

We have undertaken a detailed investigation of a complex Fermi resonance at ~ 400–450 cm^{-1} using 2D-ZEKE, and find that this appears to consist of several main contributions, each of a_g symmetry. Interestingly, although the equivalent M_{11} vibration in the related toluene molecule has been determined to be "bright",[8] the D_{11} mode here seems only to have a minor contribution to the REMPI spectrum. The major contributors to the first band of the FR feature

are from two eigenstates formed from two ZOSs: $2D_{19}$ and the D_{29} m = {0,3(+)}$^-$ vibtor level. A higher-wavenumber feature appears to be largely due to $2D_{14}$ and there is some evidence that this is weakly coupled to the other two levels mentioned. The fact that these three ZOSs are in Fermi resonance is suggested by the appearance of the 2D-ZEKE spectra, with there being a strong interaction between the D_{19} overtone and the D_{29} m = {0,3(+)}$^-$ vibtor level, but a much weaker interaction with D_{11}; other weak interactions with the D_{11}, $4D_{20}$ and D_{14}{0,6($^-$)}$^+$ levels appear to be present. To slightly higher wavenumber there is a separate band for which our best assignment is to another vibtor level, D_{18} m = {0,3(-)}$^-$; since this does not appear in the spectrum of pFT, we conclude that this may be gaining intensity from the FR, although there seems to be no clear evidence from our ZEKE spectra for this.

Acknowledgments

Table I: Calculated and experimental vibrational wavenumbers (cm^{-1}) for the S_1 and D_0^+ electronic states of pXyl, pDFB and pFT

D_i	Mulliken (D_{2h})	pXyl				pDFB				pFT			
		S_1		D_0^+		S_1		D_0^+		S_1		D_0^+	
		Calc[a]	Expt	Calc[b]	Expt	Calc[a]	Expt[c]	Calc[b]	Expt[d]	Calc[a]	Expt[e]	Calc[b]	Expt[e]
						a_1							
D_1	1(a_g)	3105		3106		3143		3118		3130		3116	
D_2	10(b_{1u})	3088		3093		3131		3108	(3098)	3105		3101	
D_3	2(a_g)	1542		1633		1519	1335	1628	1640	1528		1628	1631
D_4	11(b_{1u})	1437		1450		1422		1457		1432		1454	
D_5	3(a_g)	1176		1229		1235	1251	1350	1375	1213	1230	1311	1332
D_6	12(b_{1u})	1192		1209		1198	[1116]	1274		1185	1194	1211	1230
D_7	4(a_g)	1147		1175		1099	1015	1137	1148	1120		1158	1170
D_8	13(b_{1u})	959		965		951	937	956		954	f	969	f
D_9	5(a_g)	784		791		820	818	823	836	805	803	811	834
D_{10}	14(b_{1u})	694		693		710	[666]	726		700	f	710	f
D_{11}	6(a_g)	402	404	440	439	414	410	435	439	410	408	437	440
						a_2							
D_{12}	7(a_u)	653		994		501	583	972		588		987	
D_{13}	9(b_{1g})	546		782		429	[588]	760	726	484		770	
D_{14}	8(a_u)	201	217	349	340	97	175	360	359	172	199	356	350
						b_1							
D_{15}	15(b_{2g})	719		1005		697	670	978		706		998	
D_{16}	28(b_{3u})	640		784		667	619	864	859	651		832	
D_{17}	16(b_{2g})	502		641		567	528	710		538		671	
D_{18}	29(b_{3u})	443	400	470	476	487	438	506	508	468	435	488	
D_{19}	17(b_{2g})	203	213	232	231	279	274	289	303	243	242	266	271
D_{20}	30(b_{3u})	104	106	100	102	124	120	123	127	110	110	109	111
						b_2							
D_{21}	18(b_{2u})	3100		3104		3139		3117		3126		3115	
D_{22}	23(b_{3g})	3084		3092		3126		3109		3100		3101	
D_{23}	24(b_{3g})	1445		1399		1407	1516	1472		1427		1383	
D_{24}	19(b_{2u})	1322		1470		1397	1591	1388		1315		1470	
D_{25}	20(b_{2u})	1390		1300		1317		1311		935		1301	
D_{26}	25(b_{3g})	1277		1250		1232	[933]	1238		1255		1250	
D_{27}	21(b_{2u})	920		1133		1022	1100	1096		1053		1115	
D_{28}	26(b_{3g})	545	554	553	555	553	558	572		546	549	564	570
D_{29}	27(b_{3g})	367	370	376	378	396	403	424	430	395	399	412	416
D_{30}	22(b_{2u})	283		289		347	352	357		307	311	313	320

[a] TD-DFT B3LYP/aVTZ scaled by 0.97.

[b] UB3LYP/aVTZ scaled by 0.97; $<S^2>$ less than 0.76.

[c] From ref. 45. Square brackets indicate an assignment which was not confirmed by DF in that work. These are in poor agreement with the calculated values in the present work and so the assignment of these is uncertain.

[d] From ref. 47.

[e] Values taken from Table I in ref. 38.

[f] A value was assigned to this vibration in ref. 36, but this assignment is now thought to be questionable and will be discussed in a forthcoming paper.

Table II: Labelling of the *p*-xylene vibrational modes

Mode[a]	Mulliken (D_{2h})	Mixed (Bz)[b]	Mixed (FBz)[c]	*p*-Xylene - Varsányi[d]
		a_1		
D_1	$1(a_g)$	**2**,7a	$\boldsymbol{M_1},(M_3)$	20a
D_2	$10(b_{1u})$	**13**,20a	$\boldsymbol{M_3},M_2,(M_1)$	2
D_3	$2(a_g)$	**9a**	$\boldsymbol{M_4}$	8a
D_4	$11(b_{1u})$	**18a**,(20a)	$\boldsymbol{M_5}$	19a
D_5	$3(a_g)$	1,7a,(2,6a)	$\boldsymbol{M_6},M_9,(M_2,M_3,M_8)$	7a
D_6	$12(b_{1u})$	12,19a,20a,(13 18a)	$\boldsymbol{M_6},M_9,(M_2,M_3)$	13
D_7	$4(a_g)$	**8a**	$\boldsymbol{M_7}$	9a
D_8	$13(b_{1u})$	**19a**,12	$\boldsymbol{M_8},(M_9)$	18a
D_9	$5(a_g)$	1,6a,(7a,2)	$\boldsymbol{M_{10}},(M_9,M_2)$	1
D_{10}	$14(b_{1u})$	20a,12,(19a,13)	$\boldsymbol{M_{10}},(M_{11},M_9,M_2,M_3)$	12
D_{11}	$6(a_g)$	**6a**,7a,(2,1)	$\boldsymbol{M_{11}},(M_2,M_3)$	6a
		a_2		
D_{12}	$7(a_u)$	**17a**	$\boldsymbol{M_{12}}$	17a
D_{13}	$9(b_{1g})$	**10a**	$\boldsymbol{M_{13}}$	10a
D_{14}	$8(a_u)$	**16a**	$\boldsymbol{M_{14}}$	16a
		b_1		
D_{15}	$15(b_{2g})$	**5**,10b	$\boldsymbol{M_{15}},M_{16}$	5
D_{16}	$28(b_{3u})$	**17b**,11,(16b)	$M_{16},M_{17},(M_{15},M_{18})$	17b
D_{17}	$16(b_{2g})$	**4**,(10b)	$\boldsymbol{M_{18}},M_{17}$	4
D_{18}	$29(b_{3u})$	**16b**,11,(17b)	$\boldsymbol{M_{19}},(M_{18},M_{17})$	16b
D_{19}	$17(b_{2g})$	**10b**,4,(5)	$\boldsymbol{M_{20}},(M_{19},M_{18},M_{17},M_{15})$	10b
D_{20}	$30(b_{3u})$	16b,17b,11	$\boldsymbol{M_{20}},(M_{17},M_{15},M_{16},M_{18})$	11
		b_2		
D_{21}	$18(b_{2u})$	**20b**	$\boldsymbol{M_{21}},M_{22}$	7b
D_{22}	$23(b_{3g})$	**7b**	$\boldsymbol{M_{22}},M_{21}$	20b
D_{23}	$24(b_{3g})$	**9b**	$\boldsymbol{M_{23}}$	8b
D_{24}	$19(b_{2u})$	**18b**,(19b,14,15)	$\boldsymbol{M_{24}},(M_{25},M_{27})$	19b
D_{25}	$20(b_{2u})$	**15**,(14)	$\boldsymbol{M_{26}},M_{25},(M_{27})$	14
D_{26}	$25(b_{3g})$	**3**,8b	$M_{26},M_{25},(M_{27})$	3
D_{27}	$21(b_{2u})$	**14**,19b	$\boldsymbol{M_{28}},M_{27}$	18b
D_{28}	$26(b_{3g})$	**6b**,(8b)	$\boldsymbol{M_{29}},(M_{27})$	6b
D_{29}	$27(b_{3g})$	8b,6b,(3)	$\boldsymbol{M_{30}},(M_{27},M_{29},M_{28})$	9b
D_{30}	$22(b_{2u})$	19b,14,18b	$\boldsymbol{M_{30}},(M_{27},M_{28},M_{24})$	15

[a]Numbered according to the Mulliken convention in C_{2v} symmetry (see text), with the label in parentheses corresponding to the symmetry of the vibration within the D_{2h} point group.

[b] Normal modes of pDFB expressed in terms of those of Bz using a generalized Duschinsky approach. Those for pXyl are expected to be very similar owing to the small mass difference between 15 and 19 amu, together with the small rate of change of the vibrational wavenumbers at these masses – see ref. 14 and text.

[c] Normal modes of pDFB (D_i modes) expressed in terms of those of FBz (M_i modes) using a generalized Duschinsky approach – see text and ref. 14. Values outside parentheses have mixing coefficients > 0.2 and are termed major contributions, with bolded values being dominant contributions (mixing coefficients > 0.5). Those inside parentheses are minor contributions, and have values between 0.05 and 0.2. If there is more than one contribution of each type, these are given in numerical order. Vibrations with a mixing coefficient < 0.05 are ignored.

[d] From Ref. 16 – we have made our best attempt at determining the correspondences based on the wavenumbers cited in that work, and those we present in Table II.

Figure Captions

Figure 1: REMPI spectra of (a) *p*-xylene; (b) *p*FT; and (c) *p*DFB in the range 0 – 600 cm^{-1}. The "torsion and vibtor" region, 0-300 cm^{-1}, is discussed in detail in ref. 13 for pXyl, while that for *p*FT is discussed in ref. 38. The feature marked "ξ" contains a number of features and is discussed in detail in the text – an expanded view of this feature may be seen in Figure 5. Features marked with an asterisk are due to complexes of the parent molecule with Ar.

Figure 2: ZEKE spectra of (a) *p*-xylene; (b) *p*FT; and (c) *p*DFB in the range 0 – 600 cm^{-1}. These have all been recorded via the origin of the S$_1$ state – see text for discussion. The torsion/vibtor regions are discussed in ref. 13 for *p*Xyl, while that for *p*FT is discussed in ref. 38

Figure 3: Zero-kinetic-energy (ZEKE) spectra of *p*-xylene when exciting through the S$_1$ D_{29} vibrational energy level. Assignments are discussed in the text.

Figure 4: Zero-kinetic-energy (ZEKE) spectra of *p*-xylene when exciting through the S$_1$ D_{28} vibrational energy level. Assignments are discussed in the text.

Figure 5: Expanded view of the region of the REMPI spectrum in Figure 1(a) showing feature ξ and the two weaker bands to lower wavenumber – see text. The bands marked ξ$_A$, ξ$_B$ and ξ$_C$ are shown with a smaller step size and as a vertical trace in Figure 6.

Figure 6: Zero-kinetic-energy (ZEKE) spectra of *p*Xyl recorded via different regions of feature ξ (see Figures 1(a) and 5). An expanded view of the latter feature is presented as a vertical trace on the right-hand side of the diagram, where three regions have been identified as ξ$_A$, ξ$_B$ and ξ$_C$. Trace (a) is a longer version of the ZEKE spectrum recorded via the S$_1$ origin [see Figure 2(a)]. The ZEKE spectra shown in traces (b)–(i) were recorded at the indicated wavenumbers, with the position in the REMPI spectrum indicated by the dashed joining lines. The assignment of the spectra is discussed in the text.

Figure 7: Schematic representation of how feature ξ$_A$ (see Figure 6(a)) appears to be composed of partially-resolved rotational envelopes arising from the three main indicated contributing transitions. The blue dashed trace represents a contribution from an eigenstate dominated by D_{29} {0, 3(+)}$^-$ and the red dashed trace represents a contribution from an eigenstate dominated by 2D_{19}.

Figure 8: Expanded view of the 400–500 cm^{-1} regions of the ZEKE spectra obtained when exciting at the centres of features ξ$_A$ and ξ$_B$ – see text for assignments and discussion.
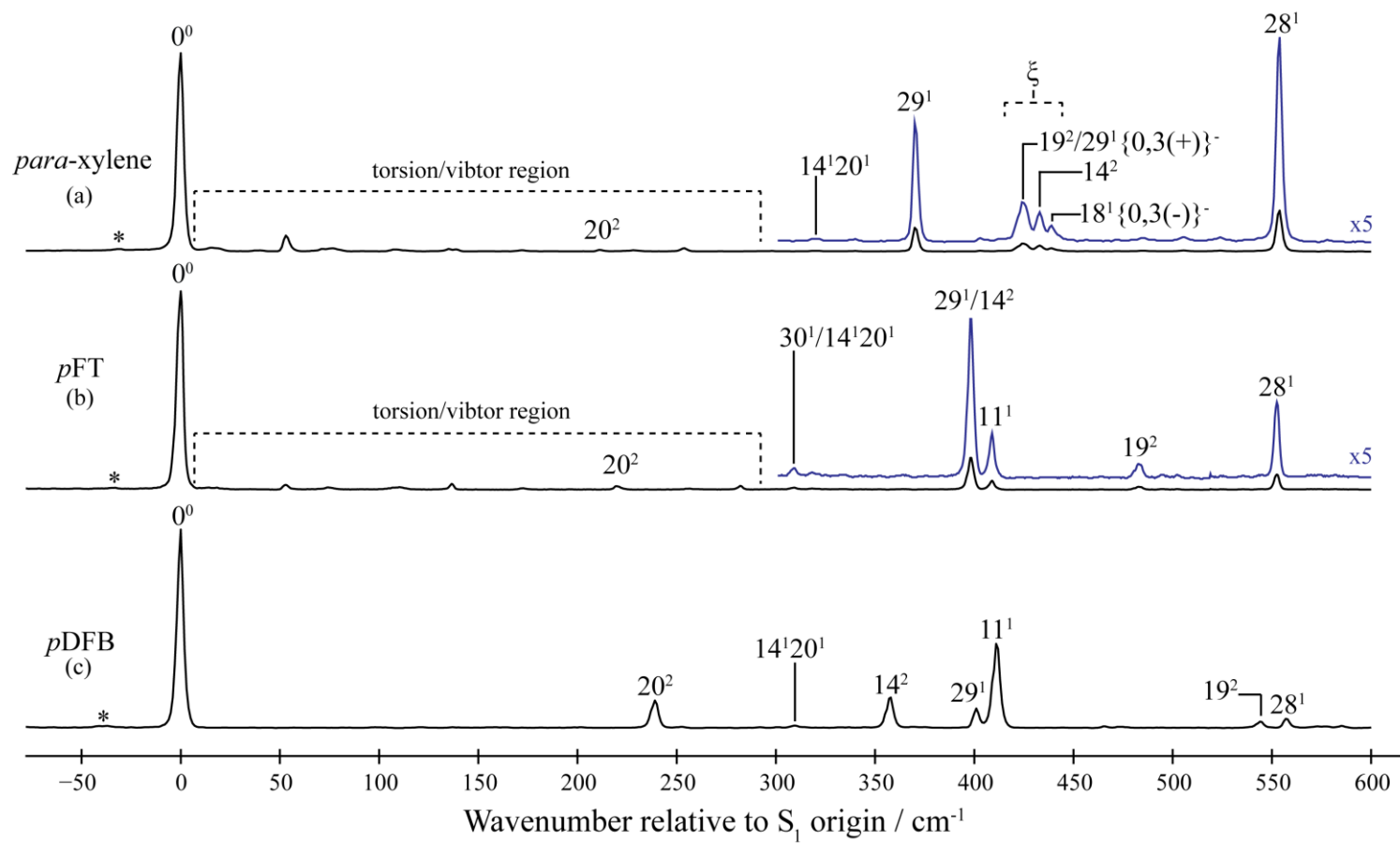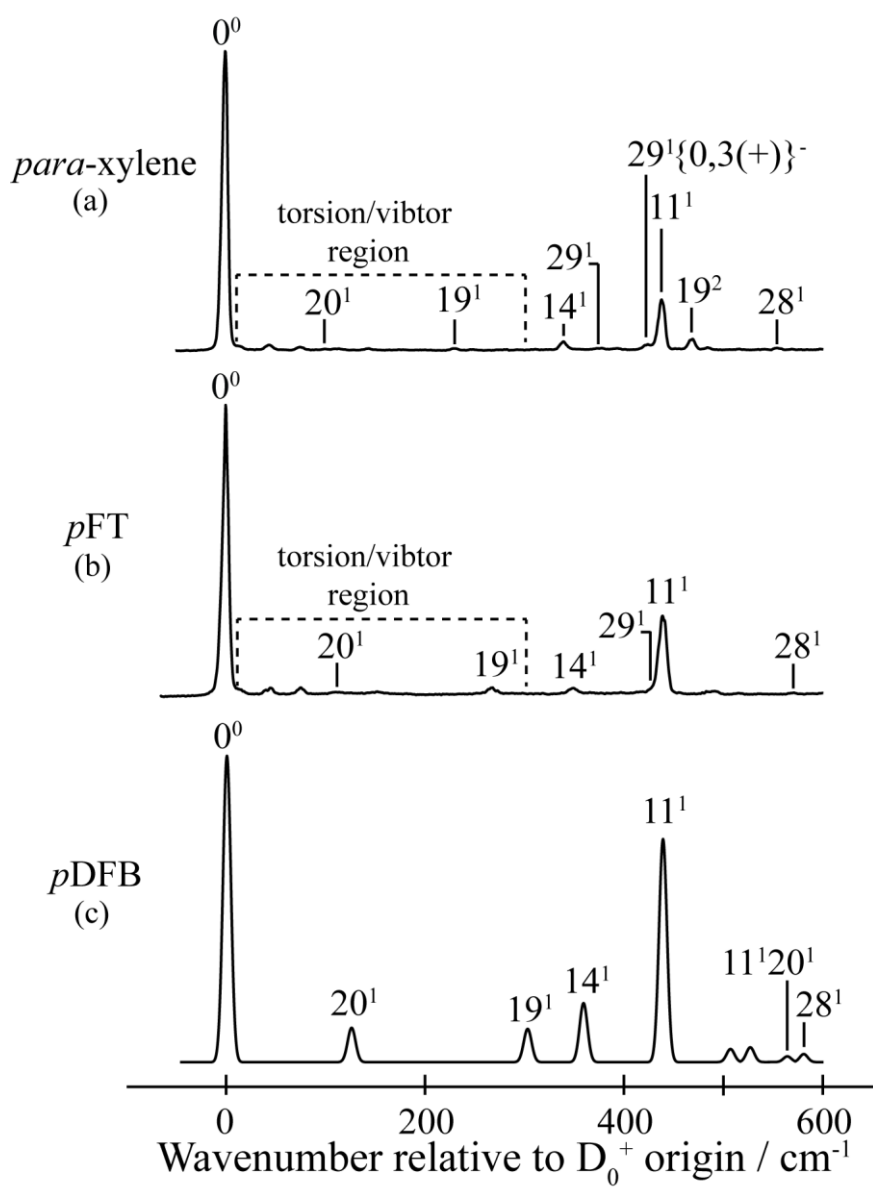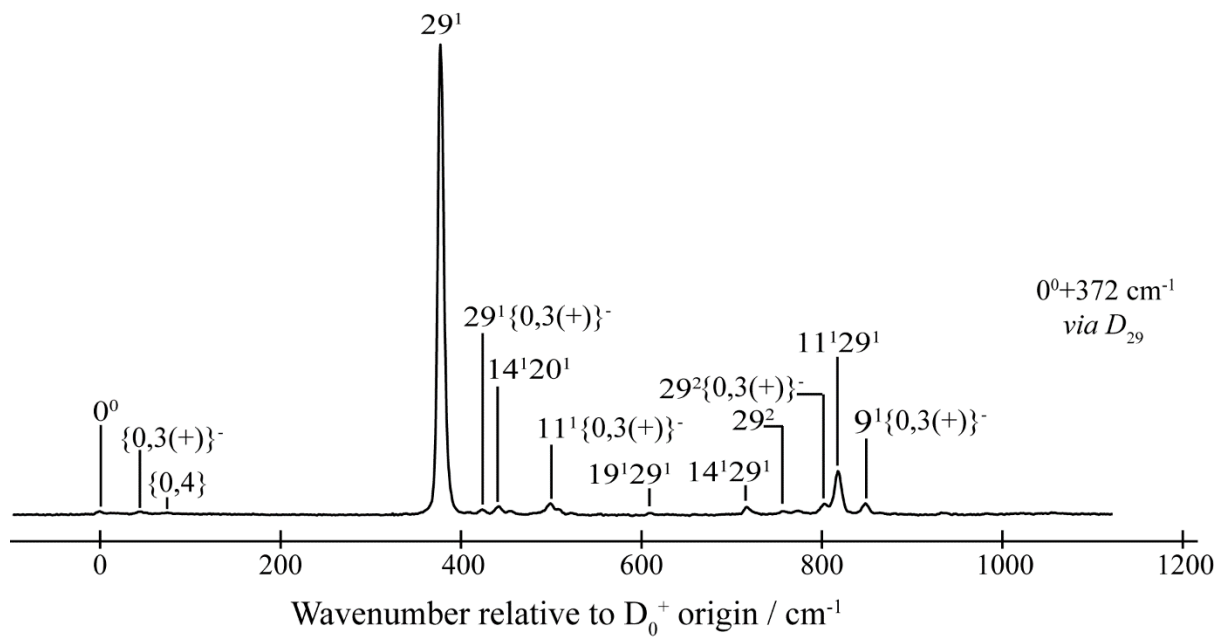
Figure 1

Figure 2

Figure 3

29^1

$29^1\{0,3(+)\}^-$

14^120^1

0^0+372 cm^{-1}
via D$_{29}$

11^129^1

$29^2\{0,3(+)\}^-$

0^0

$\{0,3(+)\}^-$

$\{0,4\}$

$11^1\{0,3(+)\}^-$

29^2

$9^1\{0,3(+)\}^-$

19^129^1 14^129^1

Wavenumber relative to D$_0^+$ origin / cm^{-1}

Figure 4

Figure 4

Figure 5

Wavenumber relative to S_1 origin / cm^{-1}

Figure 6

Figure 7

Wavenumber relative to S_1 origin / cm^{-1}

Figure 8

0^0+426cm^{-1}
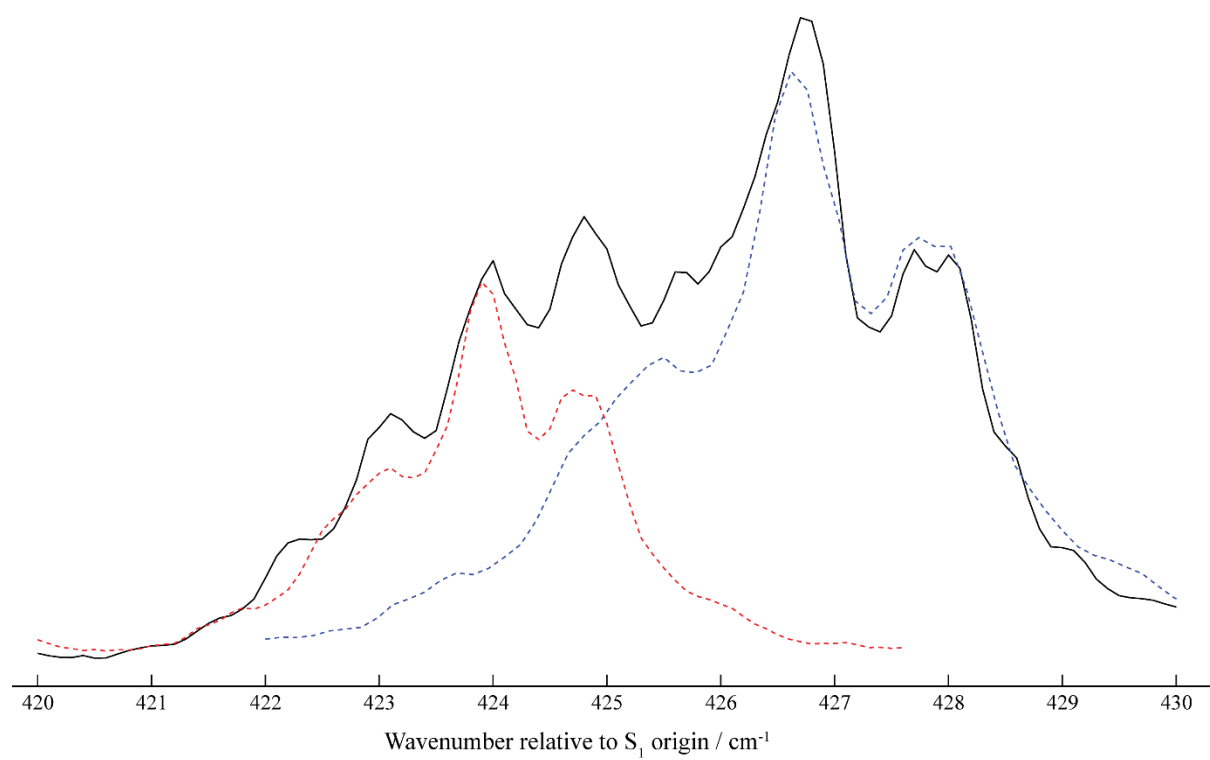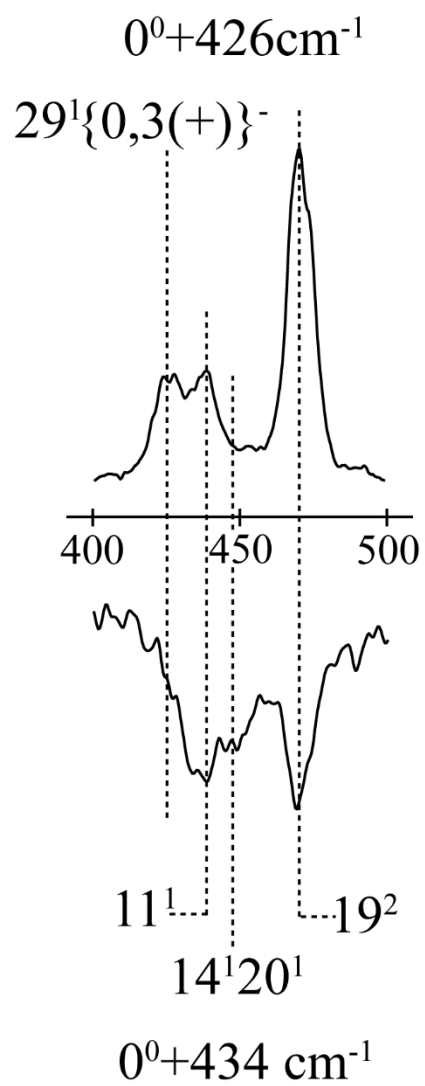
$29^1\{0,3(+)\}^-$

11^1 14^120^1 19^2

0^0+434 cm^{-1}
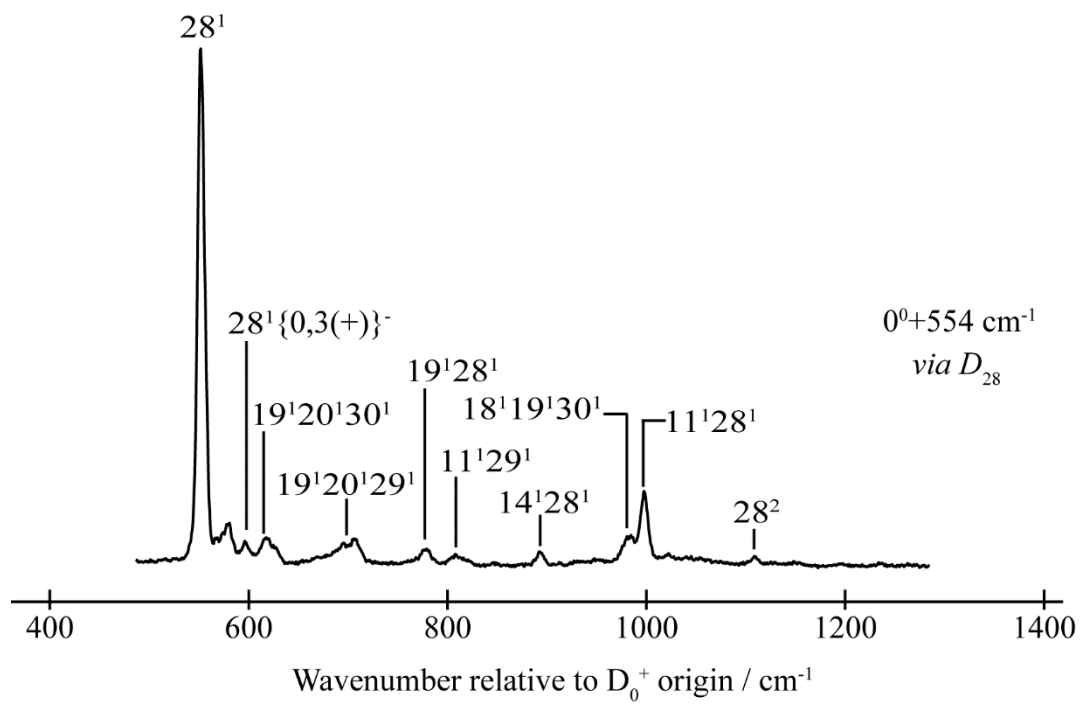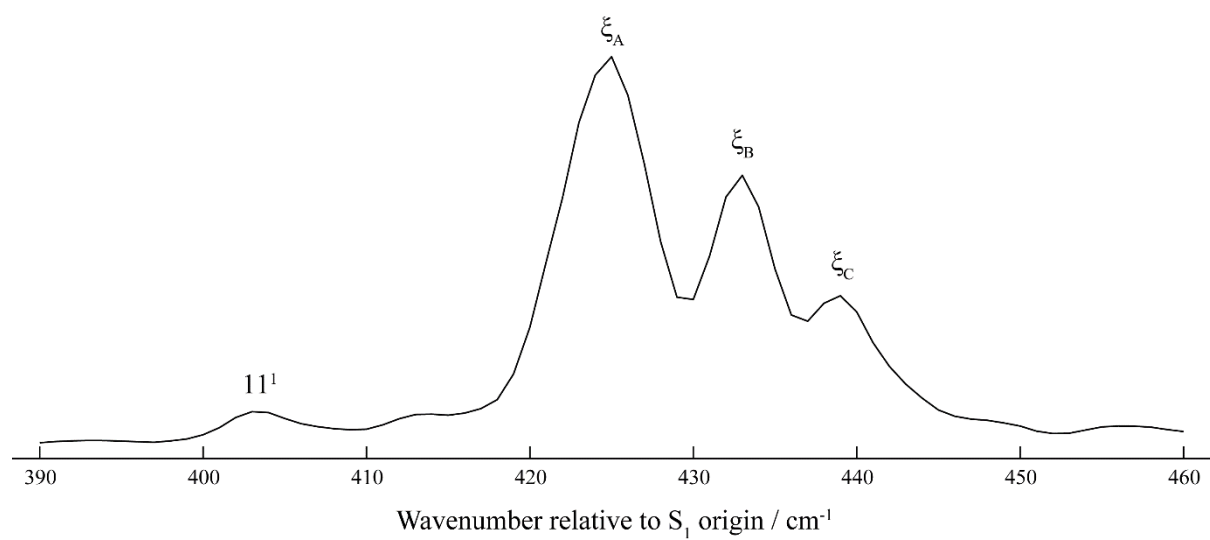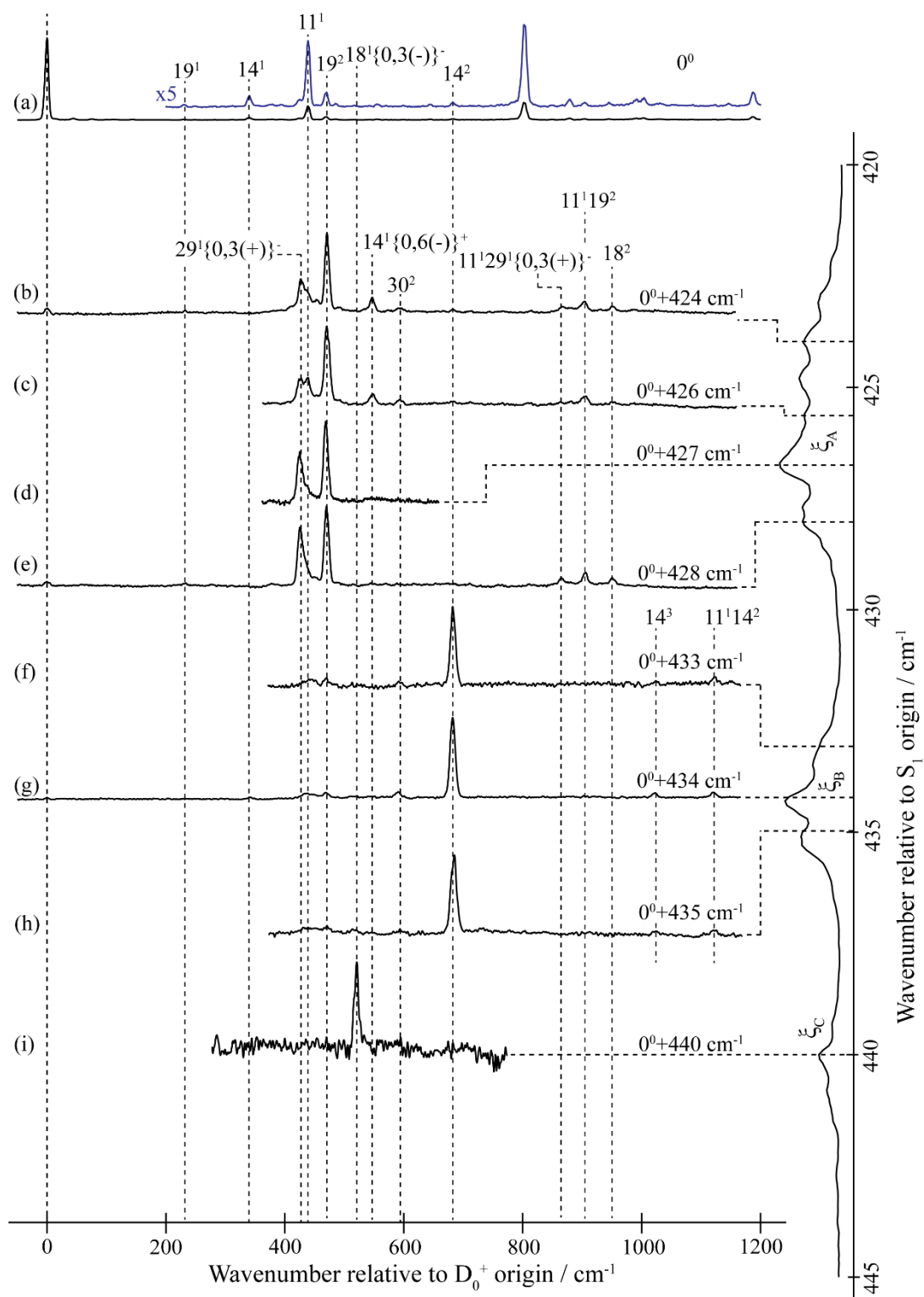
References

[1] C. S. Parmenter and B. M. Stone, J. Chem. Phys. **84**, 4710 (1986).

[2] A. M. Gardner, A. M. Green, V M. Tamé-Reyes, V. H. K. Wilton and T. G. Wright

J. Chem. Phys. **138**, 134303 (2013).

[3] A. M. Gardner, A. M. Green, V. M. Tamé-Reyes, K. L. Reid, J. A. Davies, V. H. K. Parkes and T. G.

Wright J. Chem. Phys. **140**, 114038 (2014).

[4] J. A. Davies, A. M. Green, A. M. Gardner, C. D. Withers, T. G. Wright and K. L. Reid

Phys. Chem. Chem. Phys. **16,** 430 (2014).

[5] J. A. Davies and K. L. Reid, J. Chem. Phys. **135**, 124305 (2011).

[6] A. M. Gardner and T. G. Wright, J. Chem. Phys. **135**, 114305 (2011).

[7] J. R. Gascooke and W. D. Lawrance, J. Chem. Phys. **138**, 134302 (2013).

[8] J. A. Davies, A. M. Green, and K. L. Reid, Phys. Chem. Chem. Phys. **12**, 9872 (2010).

[9] J. R. Gascooke, E. A. Virgo and W. D. Lawrance, J. Chem. Phys. **142**, 024315 (2015).

[10] J. R. Gascooke, E. A. Virgo and W. D. Lawrance, J. Chem. Phys. **142**, 044313 (2015).

[11] Y. He, C. Wu and W. Kong, J. Phys. Chem. A **107**, 5145 (2007).

[12] C. Skinnerup Byskov, F. Jensen, T. J. D. Jørgensen, and S. Brøndsted Nielsen, Phys. Chem. Chem.

Phys. **16**, 15831 (2014).

[13] A. M. Gardner, W. D. Tuttle, P. Groner and T. G. Wright, Low-wavenumber torsions and vibration-torsions in the S_1 and ground state cation of *p*-xylene investigated using resonance-enhanced multiphoton ionization (REMPI), zero-kinetic-energy (ZEKE) spectroscopy and a molecular symmetry group analysis (accompanying paper).

[14] A. Andrejeva, A. M. Gardner, W. D. Tuttle, and T. G. Wright J. Mol. Spect. **321**, 28 (2016).

[15] E. B. Wilson, Jr, Phys. Rev. 45 (1934) 706.

[16] G. Varsányi, *Assignments of the Vibrational Spectra of Seven Hundred Benzene Derivatives* (Wiley, New York, 1974).

[17] R. S. Mulliken, J. Chem. Phys. **23**, 1997 (1955).

[18] G. Herzberg, *Molecular Spectra and Molecular Structure II: Infrared and Raman Spectra of Polyatomic Molecules* (van Nostrand, New York, 1945).

[19] T. Ebata, Y. Suzuki, N. Mikami, T. Miyashi, and M. Ito, Chem. Phys. Lett. **110**, 597 (1984).

[20] P. J. Breen, J. A. Warren, E. R. Bernstein, and J. I. Seeman, J. Chem. Phys. **87**, 1917 (1987).

[21] T. G. Blease, R. J. Donovan, P. R. R. Langridge-Smith, and T. R. Ridley, Laser Chem. **9**, 241 (1988).

[22] K. Walter, K. Scherm, and U. Boesl, Chem. Phys. Lett. **161**, 473 (1989).

[23] J. I. Selco and P. G. Carrick, J Mol. Spect. **173**, 262 (1995).

[24] B. Zhang, U. Aigner, H. L. Selzle, and E. W. Schlag, Opt. Comm. **183**, 95 (2000).

[25] F. Gunzer and J. Grotemeyer, Phys. Chem. Chem. Phys. **4**, 5966 (2002).

[26] F. Gunzer and J. Grotemeyer, Int. J. Mass Spectrom. **228**, 921 (2003).

[27] B. Zhang, U. Aigner, H. L. Selzle, and E. W. Schlag, Opt. Comm. **183**, 95 (2000).

[28] A. Held, H. L. Selzle, and E. W. Schlag, J. Phys. Chem. A **102**, 9625 (1998).

[29] B. Zhang, U. Aigner, H. L. Selzle, and E. W. Schlag, Chem. Phys. Lett. **380**, 337 (2003).

[30] K. Watanabe, T. Nakayama, and J. Mottl, J. Quant. Spectrosc. Radiat. Transfer, **2**, 369 (1962).

[31] T. P. Debies and J. W. Rabalais, J. Electron Spect. Rel. Phenom. **1**, 355 (1972/3).

[32] M. Klessinger, Angew. Chem. Int. Ed. Engl. **11**, 525 (1972).

[33] T. Koenig, M. Tuttle, and R. A. Wielesek, Tetrahedr. Lett. **15**, 2537 (1974).

[34] K. Watanabe, J. Chem. Phys. **22**, 1564 (1954).

[35] C. J. Hammond, V. L. Ayles, D. E. Bergeron, K. L. Reid, and T. G. Wright J. Chem. Phys. **125** (2006), 124308.

[36] V. L. Ayles, C. J. Hammond, D. E. Bergeron, O. J. Richards, and T. G. Wright J. Chem. Phys. **126** (2007), 244304.

[37] L. D. Stewart, J. R. Gascooke, P. G. Sibley, and W. D. Lawrance, "Methyl torsion, low-frequency vibrations and torsion-vibration states in S_0 and S_1 p-fluorotoluene" (unpublished).

[38] A. M. Gardner, W. D. Tuttle, L. Whalley, A. Claydon, J. H. Carter, and T. G. Wright, J. Chem. Phys **145**, 124307 (2016).

[39] L. D. Stewart, J. R. Gascooke, A. M. Gardner, W. D. Tuttle, T. G. Wright, and W. D. Lawrance, "Torsion-vibration interactions in the S_0 and S_1 states of p-fluorotoluene and the D_0^+ state of the p-fluorotoluene cation" (unpublished).

[40] K. Okuyama, N. Mikami, and M. Ito, J. Phys. Chem. **89**, 5617 (1985).

[41] Z.-Q. Zhao, C. S. Parmenter, D. B. Moss, A. J. Bradley, A. E. W. Knight, and K. G. Owens, J. Chem. Phys. **96**, 6362 (1992).

[42] Z.-Q. Zhao, PhD Thesis, Indiana University (1992).

[43] R. A. Covaleskie and C. S. Parmenter, J. Molec. Spect. **86**, 86 (1981).

[44] M. J. Robey and E. W. Schlag, Chem. Phys. **30**, 9 (1978).

[45] A. E. W. Knight and S. H. Kable, J. Chem. Phys. **89**, 7139 (1988).

[46] D. Rieger, G. Reiser, K. Müller-Dethlefs, and E. W. Schlag, J. Phys. Chem. **96**, 12 (1992).

[47] G. Reiser, D. Rieger, T. G. Wright, K. Müller-Dethlefs, and E. W. Schlag, J. Phys. Chem. **97**, 4335 (1993).

[48] S. D. Gamblin, S. E. Daire, J. Lozeille, and T. G. Wright, *Chem. Phys. Lett.* 2000, **325**, 232.

[49] C. J. Hammond, V. L. Ayles, D. E. Bergeron, K. L. Reid, and T. G. Wright, *J. Chem. Phys.*, 2006, **125**, 124308.

[50] X. Zhang, J. M. Smith, and J. L. Knee, J. Chem. Phys. **97**, 2843 (1992).

[51] *Gaussian 09*, Revision A.02, M. J. Frisch, G. W. Trucks, H. B. Schlegel, G. E. Scuseria, M. A. Robb, J. R. Cheeseman, G. Scalmani, V. Barone, B. Mennucci, G. A. Petersson, H. Nakatsuji, M. Caricato, X. Li, H. P. Hratchian, A. F. Izmaylov, J. Bloino, G. Zheng, J. L. Sonnenberg, M. Hada, M. Ehara, K. Toyota, R. Fukuda, J. Hasegawa, M. Ishida, T. Nakajima, Y. Honda, O. Kitao, H. Nakai, T. Vreven, J. A. Montgomery, Jr., J. E. Peralta, F. Ogliaro, M. Bearpark, J. J. Heyd, E. Brothers, K. N. Kudin, V. N. Staroverov, R. Kobayashi, J. Normand, K. Raghavachari, A. Rendell, J. C. Burant, S. S. Iyengar, J. Tomasi, M. Cossi, N. Rega, J. M. Millam, M. Klene, J. E. Knox, J. B. Cross, V. Bakken, C. Adamo, J. Jaramillo, R. Gomperts, R. E. Stratmann, O. Yazyev, A. J. Austin, R. Cammi, C. Pomelli, J. W. Ochterski, R. L. Martin, K. Morokuma, V. G. Zakrzewski, G. A. Voth, P. Salvador, J. J. Dannenberg, S. Dapprich, A. D. Daniels, Ö. Farkas, J. B. Foresman, J. V. Ortiz, J. Cioslowski, and D. J. Fox, Gaussian, Inc., Wallingford CT, 2009.

[52] P. R. Bunker and P. Jensen, *Molecular Symmetry and Spectroscopy*, 2nd Ed. (NRCC, Ottawa, Canada, 1998).

[53] J. I. Selco and P. G. Carrick, J. Mol. Spect. **173**, 262 (1995).

[54] J. P. Harris, A. Andrejeva, W. D. Tuttle, I. Pugliesi, C. Schriever, and T. G. Wright, J. Chem. Phys. **141**, 244315 (2014).

[55] A. Andrejeva, W. D. Tuttle, J. P. Harris, and T. G. Wright, J. Chem. Phys. **143**, 104312 (2015).

[56] A. Andrejeva, W. D. Tuttle, J. P. Harris, and T. G. Wright, J. Chem. Phys. **143**, 244320 (2015).

[57] W. Y. Lu, Y. H. Hu, and S. H. Yang, Z. Phys. D **40**, 40 (1997).

[58] P. Butler, D. B. Moss, H. Yin, T. W. Schmidt, and S. H. Kable, J. Chem. Phys. **127**, 094303 (2007).

[59] I. Pugliesi, N. M. Tonge, and M. C. R. Cockett, J. Chem. Phys. **129**, 104303 (2008).

[60] J. G. Philis, Chem. Phys. Lett. **169**, 460 (1990).

[61] G. Herzberg, *Molecular Spectra and Molecular Structure III: Electronic Spectra and Electronic Structure of Polyatomic Molecules* (van Nostrand, New York, 1966).

[62] J. M. Hollas, *High Resolution Spectroscopy*, 2nd Ed. (John Wiley and Sons, Chichester, 1988).

[63] T. G. Wright, S. I. Panov, and T. A. Miller, J. Chem. Phys. **101**, 4793 (1995).